5. ATTITUDE DETERMINATION, CONTROL AND STABILIZATION

TABLES OF CONTENTS

List of Figures

List of Tables

5.1 Introduction

When in orbit, satellites must be oriented properly in order to implement their mission objectives effectively. Components such as antennas and cameras must be pointed within a tolerable range at a location on the Earth's surface. The attitude determination, control, and stabilization sub-system takes these factors into consideration, as well as thermal distribution and solar panel orientation.

Depending on mission objectives and payloads, attitude determination, control and stabilization (ADCS) design can be difficult. The design of an ADCS sub-system of a satellite requires careful evaluation of its payloads and their interaction with other sub-systems. Attitude determination systems must provide the accurate information necessary for one of the two following scenarios to be carried out; 1) determine the satellite's position and orientation and than make any necessary changes or corrections based on comparison to a predetermined nominal state, or 2) determine the satellite's position and orientation, only without making any changes. The control and stabilization portions of the ADCS sub-system allow any of the calculated corrections or changes to be initiated for maintaining the orbit and correcting perturbations in order to remain in the desired orientation.

In general, ADCS systems can be divided into two broad categories, active and passive. These broad categories can again be divided into several specific configurations. The first method, active spacecraft control, is often considered the most costly and complex of all and is the system used in the majority of the developed world's space endeavors. The less costly means of control is the passive regime. Passive control systems require fewer moving parts compared to active systems and have limited power requirements and thermal dissipation effects.

In the initial design process of a satellite ADCS sub-system, several things must be considered. Four of the most high-level will be identified in this report.

- Initial Attitude Acquisition is the first requirement that this system must consider. The success of a mission is highly dependent upon the ability to accurately determine spacecraft attitude.

- Spacecraft attitude control is the next logical consideration in preliminary design. The ability to maintain and correct the spacecraft attitude is vital to the successful completion of payload objectives.

- Secondary/redundant systems simply provide auxiliary control methods in case of a primary system failure.
- Contingency operations are control modes developed to perform specialized tasks not included in normal operational mode. Due to the specialized nature of these operations, they might be used only once during the life of the satellite, if at all. Such a mode could involve certain limited resources on-board the spacecraft or have negative influences on other sub-systems, thus limiting this

mode's usefulness.

5.2 Design Analysis

5.2.1 Disturbance Environment

In an Earth orbit, the space environment offers several external torques that the ADCS system must either tolerate or manage. These torques are; gravity gradient, solar radiation pressure, magnetic field effects, and aerodynamic forces. The most significant of these are gravity gradient, solar radiation, and magnetic field. Aerodynamic forces are generally not a design issue for most Low Earth Orbit (LEO) satellites above an altitude of 250 km. Disturbances are affected by the spacecraft's geometry, orientation, and mass properties. There also exists internal disturbances to the control system. Residual dipole created by the spacecraft electronics is an important consideration in disturbance torque calculation.

5.2.1.1 Gravity Gradient Disturbance

The gravity gradient disturbance is a constant torque felt by an Earth orbiting spacecraft. This disturbance is created by the finite distance between the opposite ends of the spacecraft, causing a slight difference in the force acting on those ends. The result is a torque about the spacecraft's center of mass. The gravity gradient torque can be determined by the following equation:

$$T_g = \frac{3m}{2R^3}\left|I_{zz} - I_{yy}\right|\sin(2\Theta) \qquad \text{(Equation 5-1)}^{1}$$

where,

μ = Earth gravitational constant, (3.986E14 m^3/s^2)
I_{ZZ} = moment of inertia about the z-axis (m^4)
I_{yy} = moment of inertia about the y-axis (m^4)
R = orbit radius (m)
θ = departure angle from nadir (degrees)

Figure 5-1 shows gravity gradient torques for different nadir departures over a range of altitudes. From this graph, it can be seen that the spacecraft's moments of inertia and altitude of its orbit are factors which will influence the magnitude of the torque. The following are the moments of inertia for SPARTNIK which were taken from the structures sub-system's calculations.

I_{yy} = 0.28393 kg/m²
I_{zz} = 0.35307 kg/m²

The magnitudes of these torques are all of the order of 10^{-8} N/m. The small magnitude of these torques make it easy to design around.

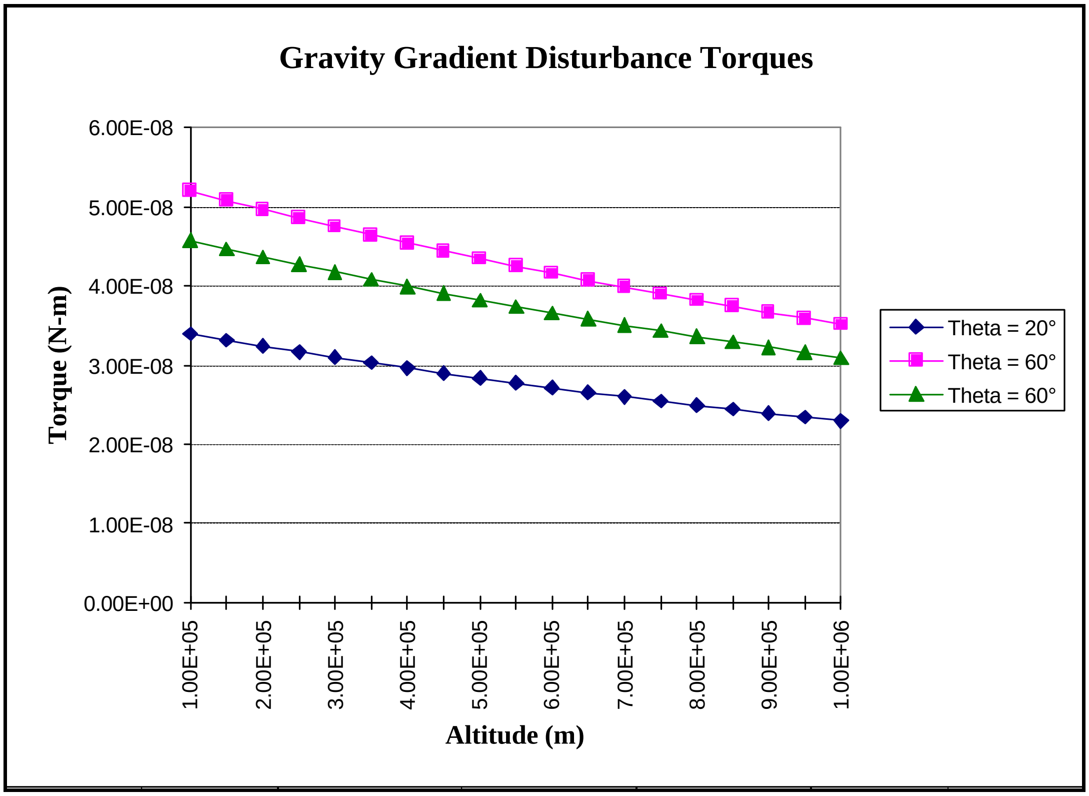

Figure 5-1 Gravity Gradient Disturbance Torque

5.2.1.2 Solar Radiation Pressure

Torque due to solar radiation pressure is caused by a difference in location of the satellite's center of pressure and its center of gravity. While in the sun, solar radiation reflected off the satellite will create a net torque about the center of gravity. On an Earth orbiting satellite these disturbances are cyclic over an orbit and are a function of the spacecraft's reflectivity.

The solar radiation torque can be calculated using the following equation:

$$T_{sp} = F\left(C_{ps} - C_g\right) \qquad \text{(Equation 5-2)}\ [1]$$

where,

$$F = \frac{F_s}{c} A_s (1 + q)\cos(i) \qquad \text{(Equation 5-3)}\ [1]$$

and,

F_S = solar constant (1358 W/m^2)
c = speed of light, (3.0E8 m/s)
A_S = surface area, (0.6993 m^2)
C_{ps} = center of solar pressure
C_g = center of gravity
q = reflectance factor, (0.6 worst case)
i = angle of incidence of the sun (degrees)

An assumption of 0.05 m for C_{ps}-C_g is used in the calculation and is typical for a small satellite.[1] Assuming a reflectivity factor q, of 0.6, Figure 5-2 shows solar radiation pressure torque over a range of incidence angles. The magnitudes of these worst case torques are all of the order of 10^{-8} m which is similar to the calculated gravity gradient torque magnitudes.

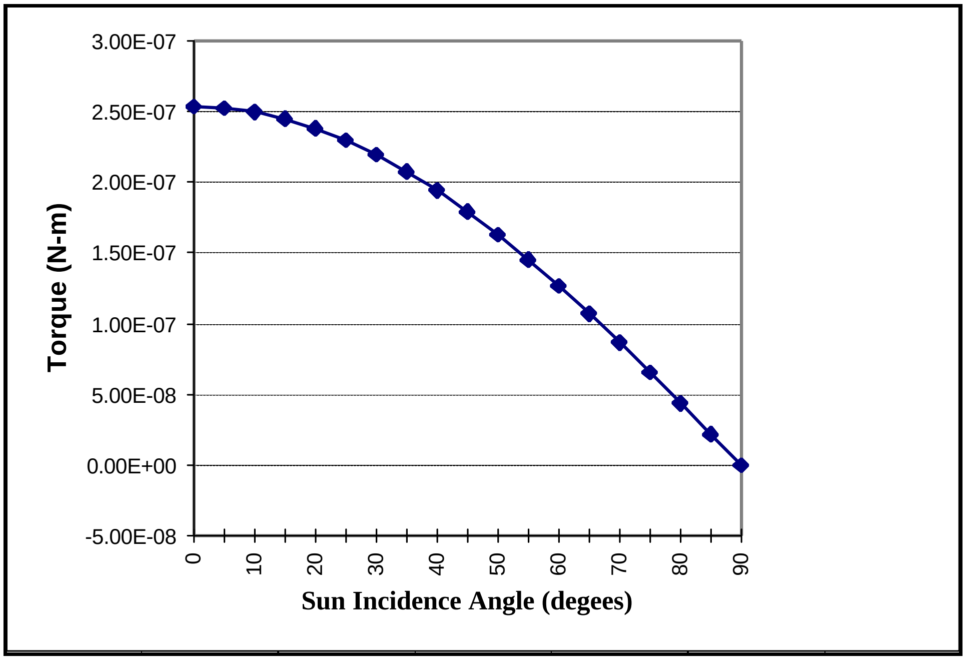

Figure 5-2 Solar Pressure Disturbance Torque

5.2.1.3 Magnetic Field Effects

Magnetic field torques are generated by interactions between the spacecraft residual magnetic dipole and the Earth's magnetic field. This spacecraft residual magnetic dipole is caused by current running through the spacecraft wiring harness. The residual dipole exhibits transient and periodic fluctuations due to power switching between different subsystems. These effects can be minimized by proper placement of the wiring harness, but during preliminary design a 1 A-m^2 residual dipole is selected as a good approximation for a small satellite.[1]

Residual dipole torques decrease with the inverse cube of the distance from the Earth's primary dipole. Figure 5-3 shows residual dipole torque magnitudes as a function of altitude.

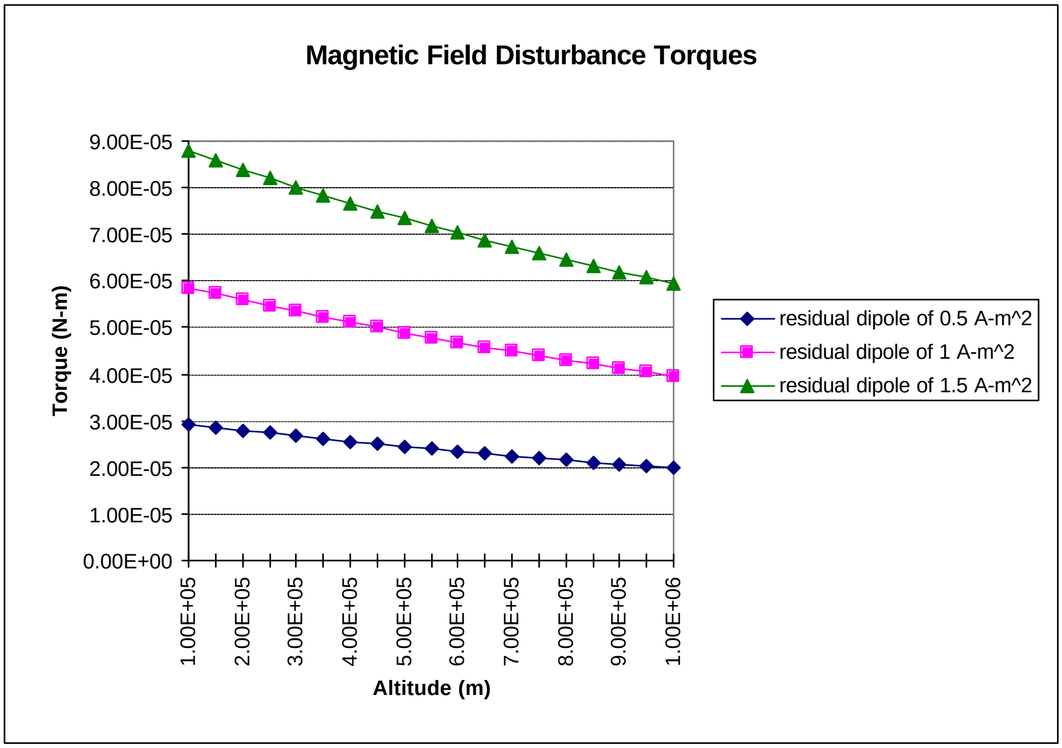

Figure 5-3 Magnetic Field Disturbance Torque

These calculations were made using the following equation:

$$T_m = DB \qquad \text{(Equation 5-4)[1]}$$

where,

$$B = \frac{2M}{R^3} \qquad \text{(Equation 5-5)[1]}$$

and,

D = residual dipole (amp-turn·m^2)
B = Earth magnetic field (tesla)
M = magnetic moment of the Earth, (7.96E15 tesla-m^3)
R = radius of orbit (m)

The magnitudes of this torque are of the order 10^{-5} N/m, which is 3 orders of magnitude larger than gravity gradient and solar pressure torques.

5.2.1.4 Aerodynamic Forces

Aerodynamic torques are due to atmospheric drag acting on the satellite. They can be quite significant, especially at low altitudes. At higher altitudes the aerodynamic torque is almost negligible. These torques can be difficult to calculate because parameters, such as cross sectional area, can change rapidly with time. Also, atmospheric density varies significantly with solar activity. Torque calculations were made using the following equations:

$$T_a = F(C_{pa} - C_g) \qquad \text{(Equation 5-6)}^1$$

where,

$$F = 0.5(rC_d A V^2) \qquad \text{(Equation 5-7)}^1$$

and,

C_d = coefficient of drag
A = cross-sectional area (m^2)
V = spacecraft velocity (m/s)
C_{pa} = center of aerodynamic pressure
C_g = center of gravity
ρ = atmospheric density (kg/m^3)

The small satellite assumption is used in determining C_{pa}-C_g.[1] Figure 5-4 shows the effects of altitude on aerodynamic torque. A logarithmic scale was necessary because of the large variation in magnitude.

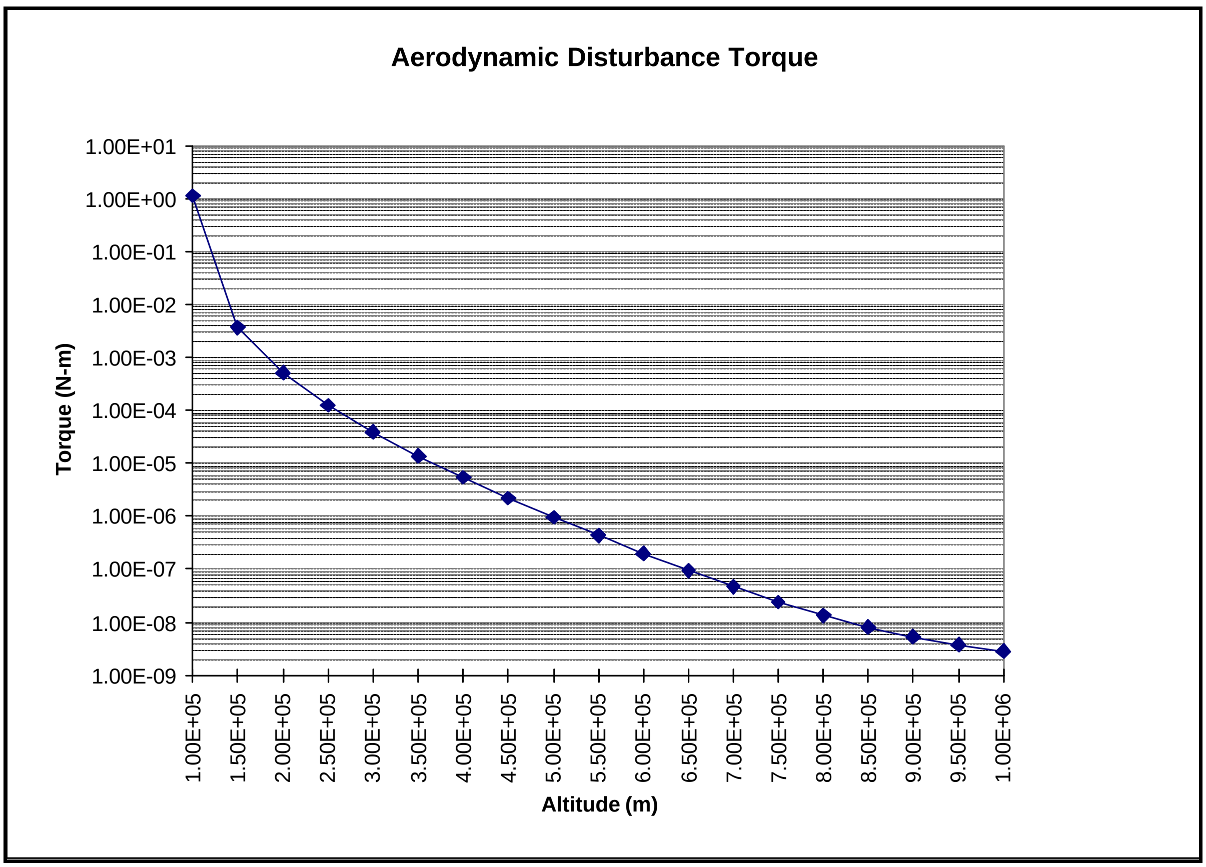

Figure 5-4 Aerodynamic Disturbance Torque

At altitudes above 600 km the torque becomes very small and at lower altitudes the aerodynamic torque is quite large with magnitudes up to 10^{-4} N/m

5.2.1.5 Total Disturbance Torque.

In order to better visualize all of the disturbance torques, they have been added together in Figure 5-5 showing the total worst case torque magnitudes over a range of altitudes. This assumes that all of the torques are acting in the same direction which is very unrealistic. The most predominant torque is created by the aerodynamic force at low altitude. At higher altitudes the total disturbance torque is sensitive to magnetic field interactions.

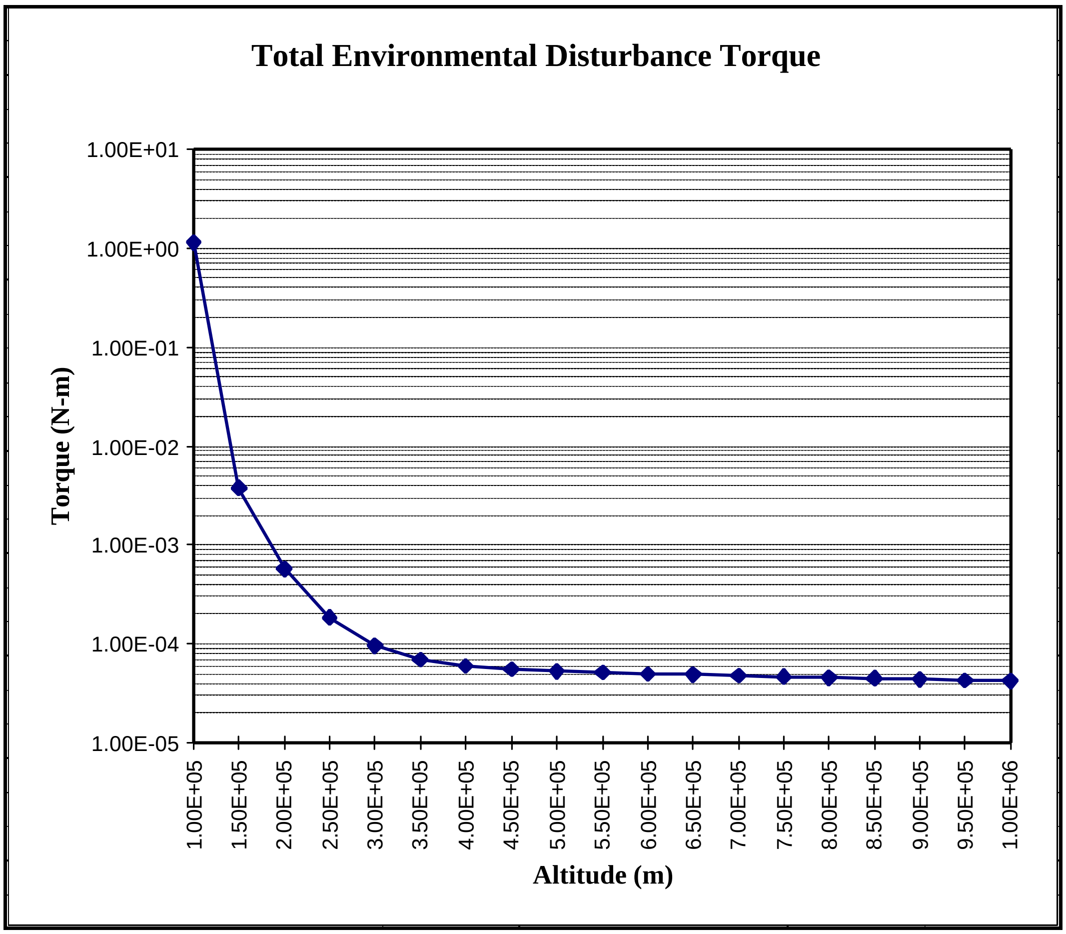

Figure 5-5 Total Environmental Disturbance Torque

One must keep in mind that these environmental disturbance models use many assumptions and are developed to show worst case expected torque magnitudes. This information can be used to assist the preliminary hardware design specifications. During the development of the SPARTNIK program, these models have been refined to show effects of disturbance interactions following more detailed analysis. This reduces the magnitude of the total expected disturbances due to torque cancellation effects.

5.2.2 Selection of Control System

A control system for SPARTNIK must be chosen in order to deal with or overcome the disturbance environment described above and allow SPARTNIK to complete its mission objectives. Control systems are divided into two types, active and passive. There are advantages and disadvantages for both. One must chose accordingly to the requirements set forth by the other subsystems. A brief description of both types of control systems follows and then the reasons for the selection of a passive subsystem will be given.

5.2.2.1 Active Control System

An active control system is one that uses movable parts that integrate with the satellite to produce changes in orientation, and give the appropriate attitude. These systems require electrical power and often computer control. Some of the components used by such control system consist of moment wheels, reaction wheels, thrusters, and others. But the integration of such control into a micro-satellite can be complicated. Usually, preliminary mission design indicates that small, unmanned low-earth orbiting spacecraft can be controlled purely by a passive control system. Even though this is the case, the possibility of using an active control system was considered.

5.2.2.2 Passive Control System

A passive control system is one which provides a controlled attitude using various methods and components that do not require moving parts. Passive control systems also do not require any electrical power, which makes them prime candidates for use in micro-satellites where power generation is minimal. Some of the components and methods of passive control are spin stabilization, gravity gradients, nutation dampers, hysteresis rods, and others. The reliability of such a control system is high. Since there are no movable parts, the chances of parts breaking, splitting or jamming are minimum. Also, gravity and magnetic fields are not going to fail, at worse their behavior will slightly deviate from the norm.

5.2.2.3 Selection of Passive Control System

The selection of the control system for SPARTNIK has primarily focused on the requirements set forth by each payload. In addition, environmental disturbances help determine minimum performance requirements that need to be achieved by the control system. These disturbances are dependent, among other things, on SPARTNIK's orbit. Although a final orbit has not been determined, analysis over a range of orbits has been performed. The candidate orbit altitudes that are being investigated are 300, 500, and 700 km with inclinations of 30, 45, 60, and 90 degrees. An extensive amount of time during the preliminary design stage and post-preliminary design report (PDR) was spent developing a parallel active/passive ADCS system. The final decision to pursue a passively spin stabilized spacecraft with a controlled tumble was made after completing preliminary research and development of an active control system incorporating the use of electromagnets. Given the complexity of such an active system, and the substantial time needed to develop and qualify the computer programs needed, the active system has been dropped from consideration. The only possibility would be to fly a portion of the active control as an experiment to qualify the theory.   Preliminary trade studies conducted are included that lead to a decision to continue with a passive control system. Additionally, the categorizing of disturbance torques experienced by the spacecraft are relevant for this system.

5.2.2.4 Design Trade Study

In the initial stages of research and development, the ideal ADCS control system was one which required little complexity and no moving parts. It was logical to make this assumption since the spacecraft is small. At this point in time, a passive control system has been selected for use on SPARTNIK.   A passive control system is commonly used on micro-satellites such as Webersat and almost all other AMSAT satellites.[2] Robert J. Twiggs from Weber State University, who worked on Webersat, was also a great and reliable source of information when considering this design.

The initial baseline option for the primary SPARTNIK ADCS sub-system was passive spin stabilization. Preliminary investigation into the hardware and design requirements was successful. The 'spinning' up of the satellite will be accomplished with eight solar pressure paddles (SPP). An explanation of how the SPP uses solar radiation pressure to develop the spacecraft spin will be given later in this document. The inclusion of permanent magnets, mounted within the spacecraft's honeycomb sides, will cause the satellite to achieve a controlled tumble of approximately two tumbles per orbit. Earth-horizon sensors will be use in conjunction with solar panel current sensors for orientation and attitude determination. After meetings with the SPARTNIK sub-system mentor, some additional information concerning the spacecraft design was brought to our attention. The technique of using passive spin stabilization brings with it two important obstacles: 1) the time required for the orbiting spacecraft to reach an equilibrium attitude and spin can be relatively long, and 2) without including permanent magnets, the spacecraft could stabilize in an attitude such that the CCD payload might never point toward the Earth, and there would be no way of making corrections to the unacceptable attitude. Additionally, it was determined that in making the initial selection of an ADCS system, key requirements of our payloads were overlooked. Given this information the spacecraft payload requirements were re-evaluated. With some industry assistance, a trade comparison conducted on passive spin stabilization vs. other methods; mainly 3-axis stabilization is shown in Table 5-1.

Table 5-1 Baseline Evaluation

	Spin Stabilization	**Other Method (3-Axis)**
Camera	- / 0	+
Radiation Sensor	0	0
Micro-Meteorite Impact Detector (MMID)	- / 0	+
Results	2 negative or 3 neutral	1 neutral or 2 plus

A plus (+) notation in the attitude stabilization column indicates that the listed payload would benefit from that type of control system. A negative (-) notation indicates the payload would be hindered by that particular system and a zero (0) indicates that the payload would neither benefit nor be hindered by that system.

Each payload was analyzed based on its requirements. Each stabilization method was then evaluated based on its ability to meet these requirements.

5.2.2.4.1 Camera

The main concern with the camera is the ability to predict where it is pointing at any given time. Although the pointing requirement of this payload is relatively loose, a more accurate knowledge of the spacecraft's attitude will afford a more precise idea of what the camera is taking a picture. The obvious solution to this problem is to allow full control over the spacecraft attitude. This is achieved through 3-axis stabilization and reduces the probability of taking unwanted pictures of deep space or of the sun.

5.2.2.4.2 MMID

Given only attitude information from the knowledge of spacecraft spin, this particular payload will provide only a "yes" or "no" answer as to whether or not an impact has occurred. The limited knowledge of attitude will only allow a rough description of the direction from which the impacting object came. The MMID was given a plus and neutral rating. Utilizing 3-axis stabilization techniques will assist in determining roughly the direction from which the micro-meteorite impacts originated.

5.2.2.5 Results of the Design Trade Study

As can be seen from Table 5-1 when the two columns are summed, the results are in favor of a stabilization method other than passive spin. The other method investigated refers to a 3-axis stabilization. Therefore, the results of this trade study show:

A. Two (2) against and three (3) neutral with regard to spin stabilization.
B. One (1) neutral and two (2) in favor of 3-axis stabilization.

From these results the decision was made to change the baseline option for the ADCS sub-system from passive spin stabilization to 3-axis stabilization. Although the same sensor configuration will be used for attitude determination, the addition of magnetorquers and a magnetometer into the control design is necessary in order to utilize the Earth’s magnetic field. This active control system is not without disadvantages. The magnetorquers require extensive orbit and magnetic field interaction simulations as well as complex control algorithms if SPARTNIK were to have complete on-board control. Another issue of concern for the magnetorquers is their need for a continuous, varying current. The torque produced is dependent upon the current supplied to the electromagnets from the power sub-system. Changes in power or current available to the magnetorquers can cause them to produce unwanted or erroneous torques which may or may not damp out the required disturbance torques. A “back-up” or contingency system was needed to supplement the active system, as long as it was simple and did not depend on power. This led to the incorporation of passive stabilization into the current active system. The passive system design must meet other specific parameters besides those listed above. One of those other parameters include the following: torques produced by the passive system must be enough to overcome the environmental disturbance torques, but at the same time cannot overcome the torques produced by the active system. The design of the passive system will be covered in more detail later in this report.

After completing several stages in the development of an electromagnetic active control system, it was discovered that the scope of implementing such a system in this project was not feasible. Consequently, the parallel design of an active and passive system has been discontinued. The SPARTNIK micro-satellite will be passively spin stabilized with a controlled tumble as described previously. Therefore, all mathematical modeling of the Earth's magnetic field and disturbance torque characterizations will still be valid. The rate of spin for SPARTNIK was decided to be 2 minutes per revolution or about 3 degrees per second.

5.2.3 Attitude Control Hardware Selection

5.2.3.1 Permanent Magnets

Permanent magnets mounted in the spacecraft are used for passive stabilization and control. They are usually used in order to make attitude determination a more reasonable task by holding the satellite in a mathematically predictable orientation. With the appropriate dipole strength and orientation, the magnets can be used to keep the satellite's positive Z axis oriented with the local Earth magnetic field vector. The magnetic dipole is shown in Figure 5-6. This control method has been used several times by AMSAT in combination with other passive control methods [2].

Satellite Magnetic Dipole

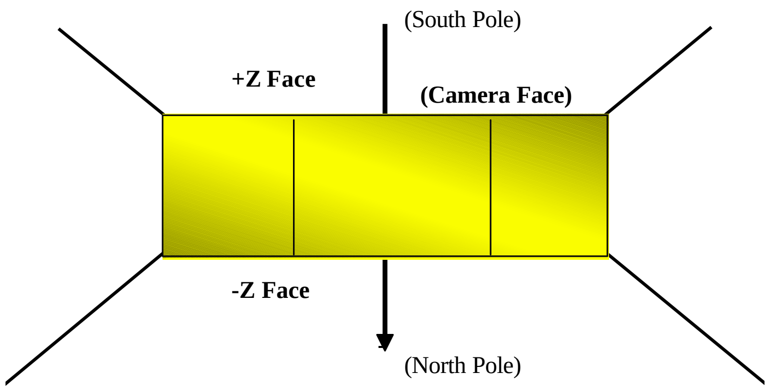

Figure 5-6 SPARTNIK's Magnetic Dipole Orientation

During the course of an orbit the satellite's orientation is influenced by the interaction of the permanent magnets with the Earth's magnetic field. As the satellite nears the magnetic equator a change in dipole orientation will cause the satellite to flip over in order to realign its magnetic dipole with the local ambient magnetic field. This "flip" effect will be repeated twice per orbit near the Earth's magnetic equator. Figure 5-7 shows the motion of the satellite over a period of one-quarter orbit.

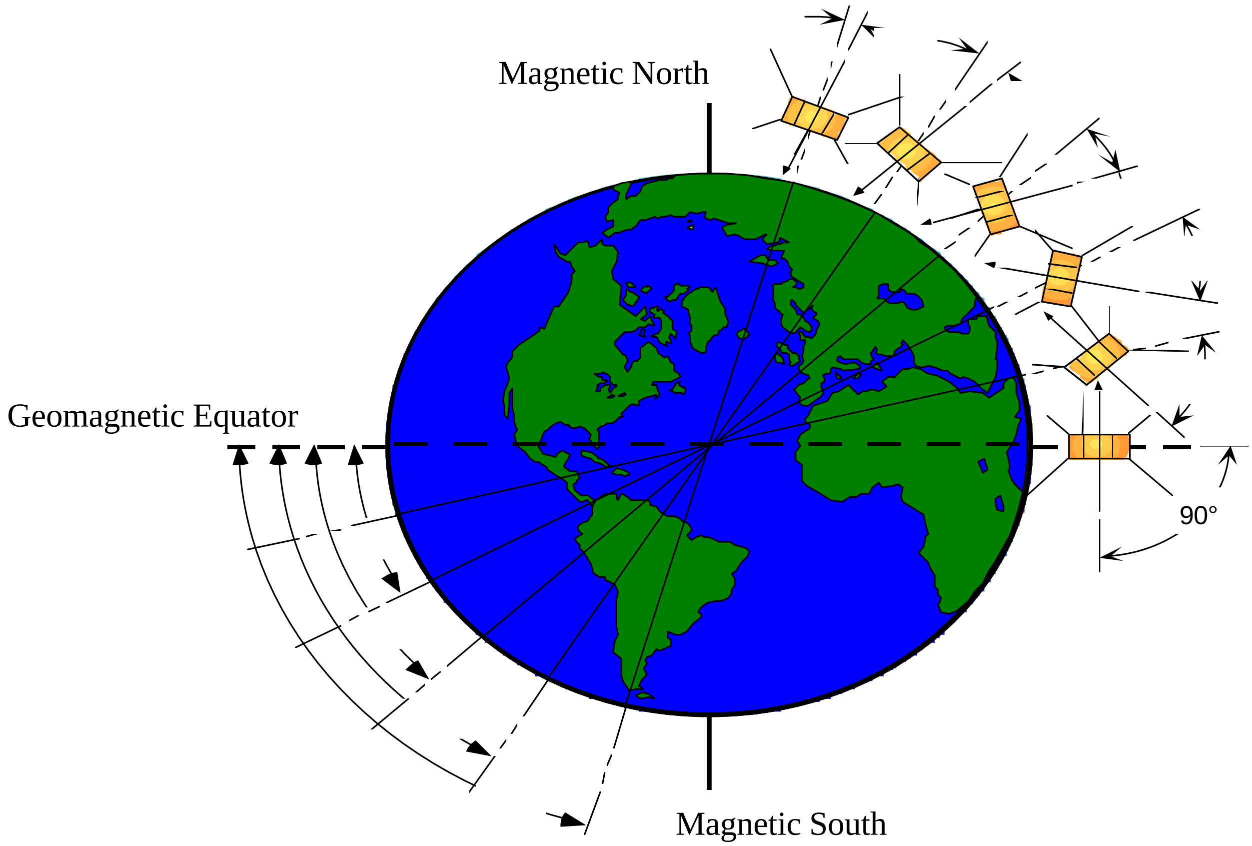

Figure 5-7 Spartnik Attitude for a Quarter Orbit

Because of the dependence of the Earth's magnetic field upon the location on an orbit, the torque created by permanent bar magnets also varies. The torque vector, **N**, generated by a magnet can be calculated using the following equation:

$$\mathbf{N} = m \times \mathbf{B} \qquad \text{(Equation 5-8)}[3]$$

where,

N = magnetic torque (dyne·cm)
m = magnet's dipole moment (EMU)
B = Earth's local magnetic field vector (Gauss)

At some intervals on an orbit the bar magnet dipoles may be parallel to the Earth's magnetic field vector, thus generating no torque.

The magnetic hardware that had been investigated included two different types of materials and two different sizes. Magnetic materials were evaluated based on their cost, magnetic strength, resistance to demagnetization, and temperature stability. The first material, Alnico-5, has been used on several small satellites including Webersat.[2] Alnico-5 is a relatively inexpensive material that has medium to high strength, very high temperature stability but low resistance to demagnetization. The Earth's relatively weak magnetic field, as compared to the proposed satellite magnets, almost negates the concern for demagnetization. Neodymium Iron Boron (NdFeB), which was the second material considered, has a very high strength, very high resistance to demagnetization, and medium to low temperature stability. This type of material will, however, retain its magnetic strength up to approximately 150°C. According to thermal calculations, the bulk temperature of SPARTNIK will not exceed this value.

Bjorn Svenssen of Dexter Magnets was consulted when the magnet size and strength was considered. He initially recommended two magnets of NdFeB, 0.75" x 0.75" x 0.6" each, located as far apart from each other to generate the largest moment arm and thus a large torque. The structure's sub-system had asked not to use these magnets due to their shape and to pursue the longer, cylinder, magnet configuration. The final selection consists of two (2) NdFeB cylinder-shaped magnets, 0.25 cm diameter by 0.25 cm height.

The magnets selected have an energy product of 35 Mega Gauss-Orested and the magnet moment was calculated to be 2.6E3 EMU. One consideration regarding using this strength of magnet is its effect on the electrical components of the satellite. However, based on discussions with the other sub-systems this will not be a concern.

5.2.3.2 Solar Pressure Paddles

The solar pressure paddles take advantage of solar radiation pressure to "spin-up" SPARTNIK for stabilization. Solar radiation pressure creates a torque on the spacecraft dependent upon the surface being illuminated. Using the same theory required for estimating this disturbance torque, we can estimate the resulting torque of the solar pressure paddles by applying the same equations. The equations 5-2 and 5-3 are repeated here for completeness.

$$T_{sp} = F\left(C_{ps} - C_g\right)$$

where,

$$F = \frac{F_s}{c} A_s (1 + q)\cos(i)$$

The four transmitting and four receiving antennas which have wavelengths of 70 cm and 2 m respectively, will serve as the "paddles" for the spacecraft. The placement and orientation of the paddles are shown in Figure 5-8. Each antenna will have a reflective coating on one side and an absorptive coating on the other. The force generated by the solar pressure varies with the reflectivity of the surface involved. A highly reflective coating will result in a greater force than a low reflective or absorptive coating. The amount of torque produced from the solar pressure paddles is the difference of the force produced by the reflective and the absorptive sides. Therefore, it is necessary to select a reflective coating with a reflectance factor, q, close to one, meaning total reflectance, and an absorptive material with a reflectance factor close to zero. The reflective material chosen was Al-FOSR, a silver coated Teflon strip only 5 mil thick with a reflectance factor of q = 0.91. Having only obtained a limited amount of Al-FOSR, a combination of this and a plain aluminum coated tape with a reflectance of q = 0.81 will be used. The absorptive side of the paddle will be anodized or painted with a space-rated flat black paint with a reflectance factor of q = 0.03. These reflectance factors were obtained from the Thermal sub-system mentor Sean Medina.

One factor to take into consideration with regard to the solar pressure paddles is the effect of thermal dissipation. As the paddles reflect the solar radiation, they emit heat as well. This effect causes an estimated 10% decrease in the net force applied on the paddles. This will result in a decrease in spin-up rate, which increases the overall spin-up time.

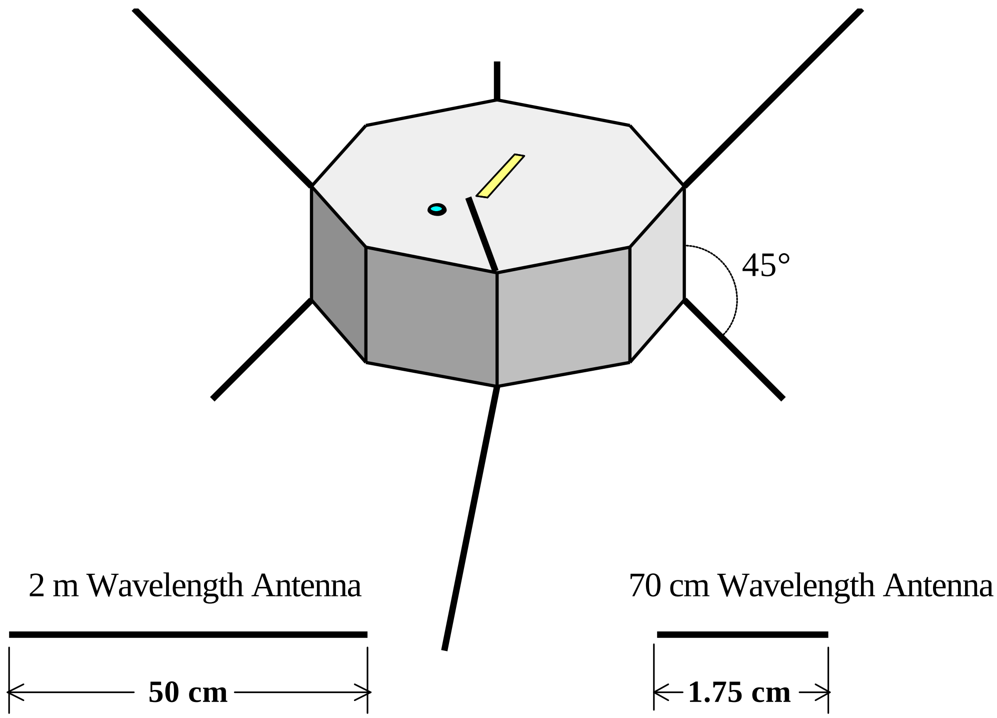

Figure 5-8 Solar Pressure Paddle Dimensions and Orientation

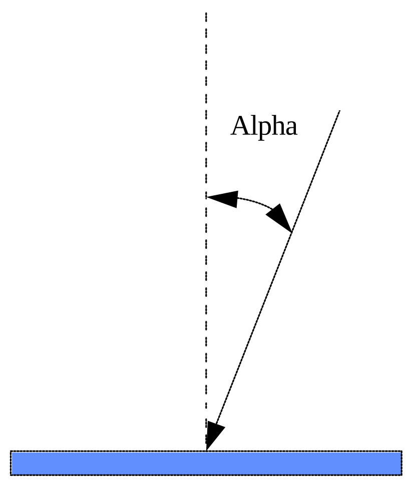

Figure 5-9 Sun Incidence Angle

Modeling the solar pressure paddles was difficult since ADCS is dependent on the sizing and mounting requirements of the antennas by the other subsystems. As seen in Figure 5-8, the antennas will be mounted one on the edge of each face at an angle of 45 degrees. The force of the solar pressure is also dependent upon the sun incidence angle on the paddles. Therefore, the orientation relative to the orbital position is very important. Figure 5-9 graphically depicts the sun orientation angle. To approximate this orientation, the following equation from Webersat's orbital dynamics was used.

$$B = 90 - \arctan(2\tan(G)) \qquad \text{(Equation 5-9)}$$ [2]

where,

B = angle variance from Nadir (degree)
G = geomagnetic latitude

This equation gives an angle as the spin axis moves away from nadir, as a result of the magnet alignment with the Earth's magnetic field. This gives the best approximation of what the spacecraft will experience on orbit since its stabilization is similar to that of Webersat. From this equation, the spacecraft and antenna geometry can be calculated and used to find the sun incidence angle relative to the surface of the paddles. Once the force and torque is calculated, a spin rate and time for stabilization can be determined. The spin rate is a function of the moment of inertia about the spin axis. A spin-up time has been calculated based on estimated values for the moments of inertia. Table 5-2 shows the solar pressure paddles performance and its approximate spin-up over a quarter orbit. . A more accurate value for the spin up time will require finalized moments of inertia.

Table 5-2 Solar Pressure Paddle Performance

Constants Used		Q reflect:	0.81	
Izz (kg m^2):	0.35307	Q absorb:	0.03	
Geomagnetic Latitude (G)	angle from nadir (B)	sun incidence angle on paddles	reflective force (N)	absorptive force (N)
90	0.00000	90.00000	1.1786E-10	6.7067E-11
85	2.50345	87.49655	1.1124E-07	6.3300E-08
80	5.03707	84.96293	2.2348E-07	1.2717E-07
75	7.62948	82.37052	3.3787E-07	1.9227E-07
70	10.31289	79.68711	4.5554E-07	2.5923E-07
65	13.12311	76.87689	5.7770E-07	3.2875E-07
60	16.10102	73.89898	7.0563E-07	4.0155E-07
55	19.29433	70.70567	8.4068E-07	4.7840E-07
50	22.75956	67.24044	9.8427E-07	5.6011E-07
45	26.56424	63.43576	1.1378E-06	6.4745E-07
40	30.78904	59.21096	1.3023E-06	7.4108E-07
35	35.52908	54.47092	1.4784E-06	8.4131E-07
30	40.89296	49.10704	1.6655E-06	9.4776E-07
25	46.99662	43.00338	1.8605E-06	1.0587E-06
20	53.94742	36.05258	2.0568E-06	1.1704E-06
15	61.81312	28.18688	2.2423E-06	1.2760E-06
10	70.57457	19.42543	2.3992E-06	1.3653E-06
5	80.07501	9.92499	2.5059E-06	1.4260E-06
0	90.00000	0.00000	2.5440E-06	1.4477E-06

As can be seen in Table 5-2, the change of the spacecraft's orientation from Nadir (B) occurring over a quarter orbit, ranges from 0 to 90 degrees. This is expected for a controlled tumble orbit. The controlled tumble is presented graphically in Figure 5-7 for one-quarter of a polar orbit.

To estimate a maximum time of spin-up, we assumed an orbit of 300 km where the solar pressure paddles will experience a minimum illumination time of 54 minutes over a 90 minute orbit. Knowing the spacecraft orientation with respect to the Earth and the solar pressure paddle mounting on the spacecraft, the sun incidence angle can be determined by simple geometry. Since the sun incidence angle on the paddles repeats four times over an orbit, the calculations from a quarter orbit allow us to see the types of forces and torques produced. Also in this table, the force resulting from the solar pressure is calculated for both the reflective and absorptive sides of the paddles using the force equation already mentioned. Table 5-3 shows the total torque produce by the reflected sides, absorptive sides, and difference between them. This torque was calculated by the equation for solar pressure torque obtained from the disturbance torques (Equations 5-2 and 5-3). Once the total torque differential between the two coated sides of the paddles is obtained the angular velocity produced can be calculated by using the moment of inertia to calculate the angular acceleration.

Table 5-3 Torque Produced by Solar Pressure Paddles

Constants Used		Q reflect:	0.81	
Izz (kg m^2):	0.35307	Q absorb:	0.03	
Geomagnetic Latitude (G)	Total Reflective Torque (N-m)	Total Absorptive Torque (N-m)	Total Torque Differential	Angular Velocity (deg./s)
90	7.021039E-09	7.235760E-08	6.533656E-08	7.576717E-04
85	7.021324E-09	7.236054E-08	6.533921E-08	7.577025E-04
80	7.021593E-09	7.236331E-08	6.534171E-08	7.577315E-04
75	7.021845E-09	7.236591E-08	6.534406E-08	7.577587E-04
70	7.022081E-09	7.236834E-08	6.534626E-08	7.577842E-04
65	7.022301E-09	7.237061E-08	6.534831E-08	7.578080E-04
60	7.022505E-09	7.237271E-08	6.535020E-08	7.578299E-04
55	7.022692E-09	7.237464E-08	6.535195E-08	7.578502E-04
50	7.022863E-09	7.237640E-08	6.535354E-08	7.578686E-04
45	7.023018E-09	7.237800E-08	6.535498E-08	7.578853E-04
40	7.023157E-09	7.237942E-08	6.535627E-08	7.579003E-04
35	7.023279E-09	7.238068E-08	6.535740E-08	7.579134E-04
30	7.023385E-09	7.238177E-08	6.535839E-08	7.579249E-04
25	7.023474E-09	7.238270E-08	6.535922E-08	7.579345E-04
20	7.023548E-09	7.238345E-08	6.535990E-08	7.579425E-04
15	7.023605E-09	7.238404E-08	6.536043E-08	7.579486E-04
10	7.023645E-09	7.238446E-08	6.536081E-08	7.579530E-04
5	7.023670E-09	7.238471E-08	6.536104E-08	7.579556E-04
0	7.023678E-09	7.238480E-08	6.536112E-08	7.579565E-04
			1/4 Orbit =	1.439932E-02
			Total Orbit =	5.759728E-02

The angular velocity resulting from the total torque is accumulated over a quarter orbit since the solar radiation pressure is constant while the paddles are being illuminated. This allows for a continuous torque at some magnitude being produced by the paddles, therefore the angular velocities will "build up". While the spacecraft is in eclipse, the solar pressure paddles will not be able to produce any torque, so the spacecraft will not gain angular velocity. The time necessary to spin up to 0.5 rev/min or two minutes per revolution, can be calculated by looking at the accumulation of angular velocities over several orbits. The total angular velocity accumulated over one orbit will be the same as the angular velocity accumulated in the second orbit considering the paddles have a minimum illumination time on orbit. The sum of these orbits will eventually give the desired angular velocity of 3 degrees per seconds. Table 5-4 gives the time required to spin-up to this rate.

Table 5-4 Spin-up Time

SPIN-UP TIME	**TO 2 MIN/REV**
TIME (days) =	6.98489772

Appendix 5-A gives some calculations of the time required for the SPP to stabilize the spacecraft from a five degree per second counter-clockwise rotation about the spin axis, and to spin up the spacecraft to a two minute per revolution clockwise rotational rate.

5.2.3.3 Hysteresis Rods

The solar pressure on the paddles is constant as long as the spacecraft is out of eclipse. This causes the spacecraft to spin-up continually until it is spinning at a higher than desired rate. Therefore, hysteresis rods are used to keep the spin from increasing past our nominal rate. Several of the AMSAT satellites have used hysteresis to control spin rate. Robert Twiggs recommended use of four to six iron rods aligned in the x-y plane of the spacecraft. For design considerations, the hysteresis rods used to control our spin will be 14 inches long and 0.14125 inches in diameter. The following includes the theory behind hysteresis rods and how they work.

The hysteresis rods are composed of 49 percent hyperm steel and are hydrogen annealed. These rods generate "eddy currents" when passing through a magnetic field. Eddy currents are currents induced in a material to oppose motion or movement in any one direction. The rods have a very small resistivity, which can be calculated as having a resistance dependent on its length and cross-sectional area. When the iron rods move through the Earth's magnetic field an electromotive force (emf) is induced:

$$\varepsilon = (\mathbf{B})(L)(v) \qquad \text{(Equation 5-10)}^{4}$$

where,

- ε = electromotive force (emf)
- **B** = Earth's magnetic field (Gauss)
- L = length of rod (m)
- v = velocity of rods (m/s)

The speed of the rods traveling through the Earth's magnetic field is equivalent to the spin rate of the spacecraft. The emf induced will create an eddy current which can be calculated by the following:

$$\boldsymbol{i} = \frac{e}{\boldsymbol{R}} \qquad \text{(Equation 5-11)}^{4}$$

where,

- *i* =current (amps)
- ε = Electromotive force (emf)
- R =resistance of iron (ohms)

Once the current is induced in the rods, a force is generated that will oppose the motion or velocity experienced. That is, since the magnets keep the spacecraft aligned perpendicular to the magnetic field, the direction of the force can be seen acting in the opposite direction.

$$F = i(L \times \mathbf{B}) \qquad \text{(Equation 5-12)}^{4}$$

where,

F	= opposing force (EMF)
i	= current (amps)
L	= length of rod (m)
B	= Earth's magnetic field (Gauss)

This opposing force will increase with an increase in the spacecraft rotational velocity until an equilibrium is reached and the satellite's angular acceleration will be zero. The hysteresis rods are mounted along the bottom side of the power sub-system tray in the x-y plane, perpendicular to the spin axis, as show in Figure 5-10.

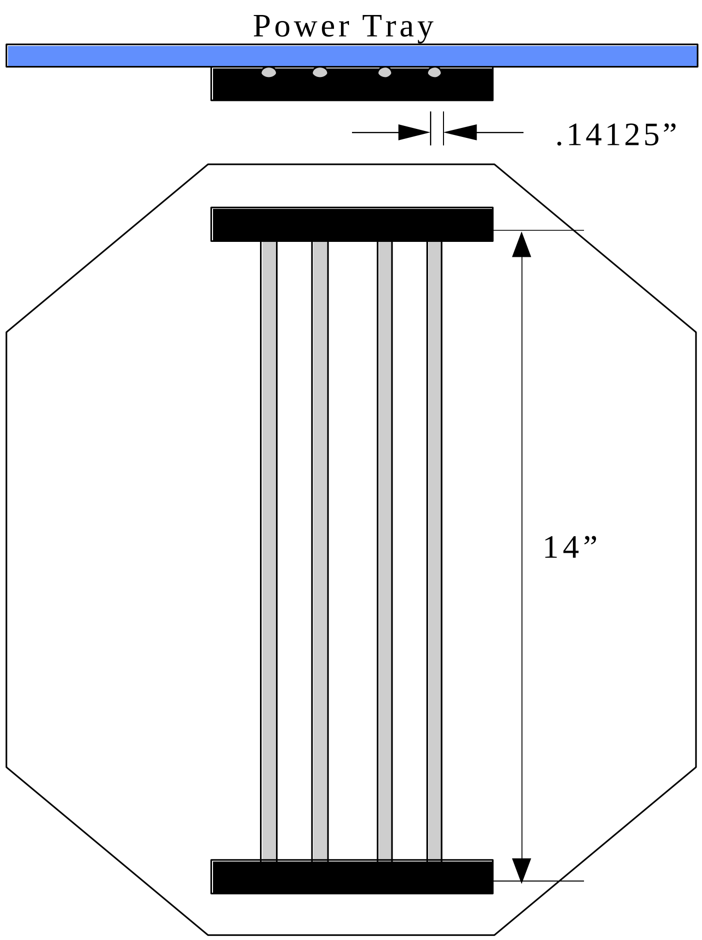

Figure 5-10 Hysteresis Rod Configuration

5.2.3.4 Nutation Damper

The nutation damper consists of a viscous ring damper mounted on the upper inside surface of the spacecraft, perpendicular to the spin axis. A viscous ring damper is a simple device that uses fluid friction to dissipate energy from a nutating body.

The ring consists of thin walled tubing that is rigidly mounted to the spacecraft body. The tubing is partially filled with a viscous fluid. When the spacecraft is turning about its spin axis, centripetal force causes the fluid to push against the inside of the thin walled tubing. This normal force of the wall combined with the viscosity of the fluid creates a frictional force that opposes motion of the fluid. After initial spin-up, the frictional force will eventually bring the fluid up to the same velocity as the thin walled tubing. The fluid will not continue to increase in velocity because the frictional force would change direction, opposing any increase.

In order to understand the nutation damping process, consider one cross section at a fixed point on the ring damper which is rotating with the spacecraft. When the spacecraft is not nutating the fluid remains at rest - pushed against the wall by the constant centripetal force. (Figure 5-11a) When the spacecraft is nutating, the off axis spin combined with precession will cause this fixed point in the cross section to move up and down. This motion disturbs the fluid from its static state causing frictional forces that oppose the vertical motion, Figure 5-11b.

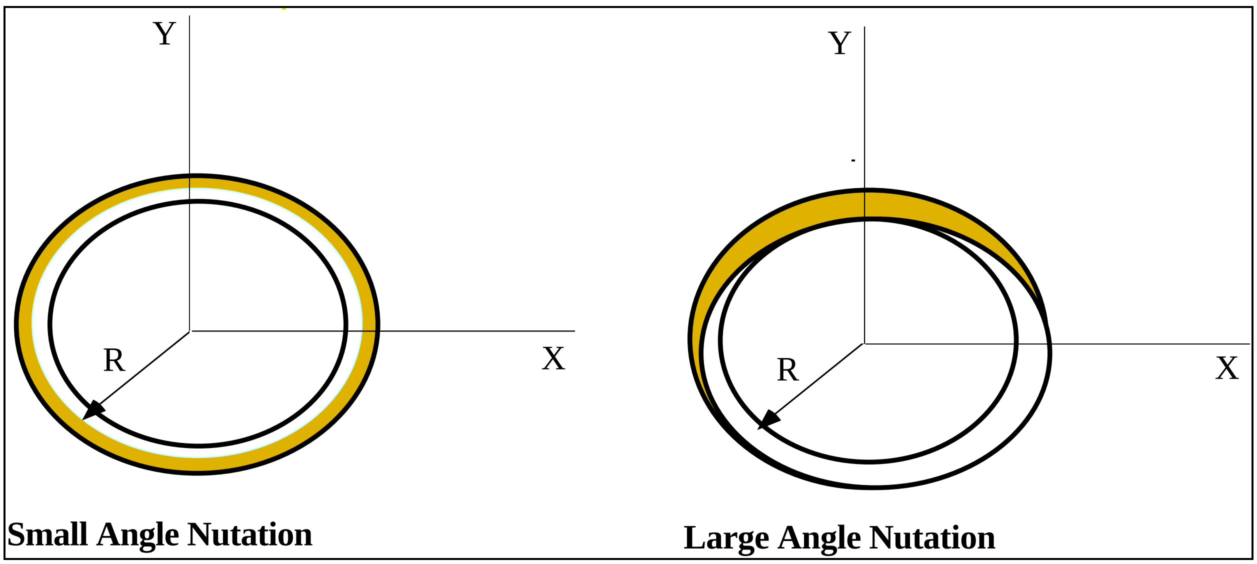

Figure 5-11a Figure 5-11b

The viscous ring damper will be 14.875 inches in diameter, and the thin walled tubing cross section is 3/8 inch in diameter. The thin walled tubing is made of 98% aluminum mixed with other elements including: 0.06% silicon, 0.7% iron, 0.05%-0.2% copper, 1.0%-1.5% magnesium, and 0.1% zinc. The tubing has a 12.9 coefficient of thermal expansion. As a pressure vessel the tubing can withstand 9498 psi before yielding. The pressure vessel will only experience 14.7 psi because the viscous fluids, air and oil, will be at atmospheric pressure while the outside of the tube will be a vacuum. The tubing will be sealed with an ultra-high leak proof flair fitting. The pressure calculations can be found in Appendix 5-H.

The viscous fluid will be synthetic 10/40 weight motor oil. This fluid was chosen for its specially formulated properties, which include nearly constant viscosity over wide temperature ranges and favorable thermal characteristics that keep it from solidifying at low temperatures.

The centripetal force pushing the fluid against the tubing wall will be 0.0225 lbs. This amount of force will give an expected frictional force of about 1.124e-4 lbs. This force may be small, but to give some idea of how effective it is, this force will bring the fluid from rest up to the target spin rate (0.5 rev/min) in about 42 seconds.

Table 5-5 Nutation Damper Specification

Spin Rate	0.5 rev/min
Hoop Radius	7.44 in
Skin Friction	0.005
Fluid Mass	0.437 slugs
Fluid Volume	2.53 in^3
Centripetal Force	0.0225 lbs
Frictional Force	1.124e^{-4} lbs
Spin Damping Torque	7.375e^{-5} lb-ft

5.2.3.5 Infrared Sensors

The Earth-Horizon sensors are infrared detectors, which will be used to determine SPARTNIK's pointing relative to the Earth. These sensors were obtained from Radio Shack (Part # 276-145), and will be used for the following purposes:

1) As a way to determine when the Earth is in the viewing area of the camera.

2) As support for our attitude determination by Earth sensing.

The Earth-Horizon sensors consist of two photo transistors whose output is a function of infrared radiation. The infrared detectors will be located on the top face of the spacecraft, one on each side of the camera lens. The sensors will be mounted inside of the aluminum honeycomb structure with an opening of approximately 1 mm through the outer aluminum plate while the sensor circuitry will be located on the main CPU board. The purpose of a small aperture is to aid in limiting the field of view of both sensors. By mounting these sensors in such a way, the Earth will be the only source of infrared radiation which will occupy the sensors combined field of view of approximately 40 degrees. This is known since at an altitude ranging from 300 to 700 km, the Earth will occupy between 145 to 130 degrees field of view of the camera's face as it points towards Earth. A diagram of the proposed configuration is shown in Figure 5-12.

Similar to the solar arrays, the Earth-horizon sensors must be calibrated before launch to determine the sensor output as a function of infrared radiation and incidence angle. Once the Earth enters the combined field of view, both sensors will be triggered to register a maximum output. During periods when both sensors are reading a maximum voltage output, it is logical to

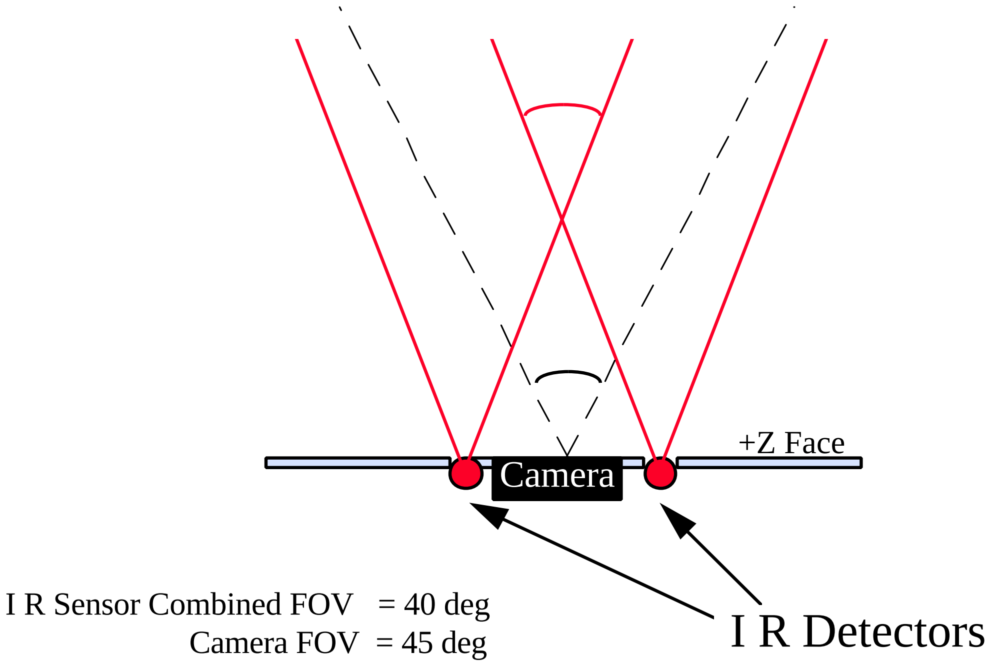

Figure 5-12 Earth Horizon Sensor (EHS) Detection Placement

assume that the Earth is also in the field of view of the camera. Considerations must also be given to the infrared radiation emitted by the moon and the sun, therefore preliminary testing of the detectors is required. The testing of the infrared sensors is discussed later in this document. The type of infrared sensor selected detects infrared radiation with a wavelength of 1 micron. This is a major drawback since the infrared radiation of the Earth has a wavelength of approximately 15 microns[4], in this case the sensors will only be able to give binary readings of on or off to indicate whether or not the sensors are being illuminated.

Once SPARTNIK is in orbit the data sampled by the sensors will serve as telemetry data for the spacecraft. The way in which these sensors will operate over an orbit is as follows:

1) On initial orbit insertion the CPU will be taking sensor reading six times per second.

2) Once on orbit the CPU will collect data to be used in the Attitude Determination Algorithm (see Algorithm description on p.46).

3) After stabilization, when a picture is to be taken, the sensors will be activated for the CPU to begin collecting data.

4) Once the two sensors are reading a maximum output and the values correspond to an angle that is known to be within the field of view, a picture or pictures of the Earth can be taken. (Note: The CCD is not limited to operating only when the sensors give an "on" reading.)

5) Once the picture or attitude determination readings have been taken, the sensors may be turned off, or remain on for the data collection or sensor testing and calibration.

5.2.4 Passive Control System Modeling

5.2.4.1 Earth's Magnetic Field Interaction Modeling

A six degree of freedom integrated model was developed in C, in order to determine the orientation of the satellite at different latitudes. This model takes into account the predicted two tumbles per orbit generated by the spacecraft's attitude control magnets. The program was developed by Darren Dow from the software subsystem. This model incorporates the gyroscopic rigidity of the spinning spacecraft. All of the simulations are performed over one polar orbit. The goals of this model are as follows:

1) Show what latitudes would be available for picture taking.
2) Determine the optimum angle for camera mounting.
3) Show the amount of nutation that could be expected during a magnetic field imposed "flip" of the spacecraft.

Using Quick, an application program, a routine was set up to calculate the magnetic field vector at every second along several different 90 minute orbits. The data acquired from these magnetic field simulations was then combined with a C program which integrates the interactions between the spacecraft's magnets and the Earth's magnetic field. The accumulation of torques and angular accelerations created by such interaction are then used with the satellite's equations of motion to predict the satellite's attitude over different orbits. The model shows how the nutation angle varies with respect to the bar magnet's strength as well as the orbit inclination. In order to understand how the magnets interact with the Earth's magnetic field a brief discussion of the field is included.

5.2.4.1.1 The Earth's Magnetic Field

The Earth's magnetic field is simply characterized by a magnetic dipole, such as that produced by a current loop or a sphere of uniform magnetization. Originating within the earth, this magnetic dipole is offset from the Earth's center, and is fixed in the rotating frame of the Earth with a slight variation of about 0.19° per year westward and 0.23° per year northward.[3]

Secondary current loops produce local magnetic dipoles in the magnetic field. These secondary dipoles interact with the primary dipole to produce local anomalies, giving the magnetic field a multipole nature. Secular drift is caused by the creation and decay of secondary current loops.

The higher order multipole effects interact in a complicated manner within the Earth's primary dipole, but luckily it can be modeled. To model such phenomena, an equation for the Earth's magnetic field potential, which is expressed in spherical harmonics, is used. This equation is the following:

$$u(\boldsymbol{r}, q, f) = \boldsymbol{a} \sum_{\boldsymbol{n}=1}^{\boldsymbol{k}} \left(\frac{\boldsymbol{a}}{\boldsymbol{r}}\right)^{\boldsymbol{n}+1} \sum_{\boldsymbol{m}=0}^{\boldsymbol{n}} \boldsymbol{g}_{\boldsymbol{n}}^{\boldsymbol{m}} \cos \boldsymbol{m}(f) + \sin \boldsymbol{m}(f) \boldsymbol{P}_{\boldsymbol{n}}^{\boldsymbol{m}}(f) \quad \text{(Equation 5-13)}^{3}$$

where,

a	= equatorial radius of Earth (km)
r	= geocentric distance (km)
?	= coelevation (degrees)
?	= east longitude from Greenwich (degrees)
gn	= Gaussian coefficient
Pn	= Gaussian coefficient

The Gaussian coefficients, g_n and P_n, must be determined using least squares fit on collected magnetic field data. These coefficients are updated frequently by the U.S. Geophysics Magnetic Survey and have been verified to be quite accurate by magnetic field measurements obtained from satellites.

The primary magnetic field harmonic is called the dipole. The second and third order harmonics are called the quadrupole and octupole, respectively. The strength of the magnetic field decreases with the inverse cube of the distance from the center of the dipole. The quadrupole decreases with the inverse fourth power and the higher degree poles decrease even more rapidly. Therefore, use of the primary dipole alone is a good approximation for preliminary field strength approximations. Examples of the Earth's magnetic field intensity over time are shown in Figure 5-13. The data are output in Cartesian coordinates with respect to the center of the Earth.

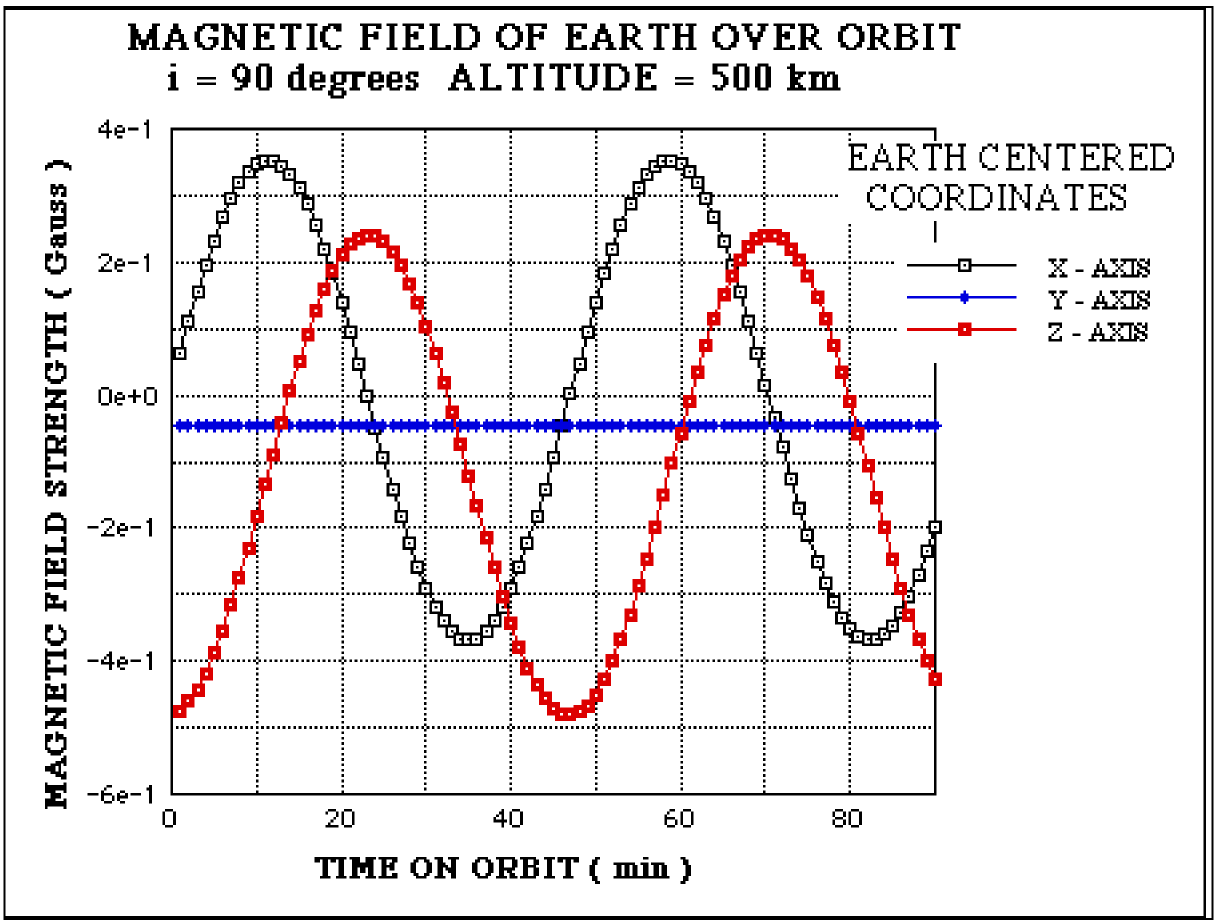

Figure 5-13 Magnetic Field Strength over Orbit

5.2.4.1.2 Results

Some preliminary results can be observed in Figure 5-14 and Figure 5-15. These graphs were generated by using a 10 Amp-m^2 magnet strength configuration. Magnets of this strength are weaker than planned in order to show worst case results of magnetic orientation control. The spacecraft's orientation angles over the period of half an orbit are shown in Figure 5-14. Lambda (λ) is the angle between the rotating body frame z-axis(spin axis) and the spacecraft non-rotating z-axis. Phi (ϕ) is the angle between the rotating body frame x-axis and the spacecraft non-rotating x-axis. Theta (θ) follows from above; obeying the right hand rule. The most important angle to consider is Phi, since it shows the orientation of the satellite's spin axis over half an orbit. From Figure 5-14, it can be noticed that the dynamic model follows the predicted two tumbles per orbit. Figure 5-15 shows the worst case expected nutation angles over half an orbit. This graph shows a maximum worst case nutation angle of 25° for a period of about 70 seconds. The magnitude of these nutation angles can be greatly reduced with the use of stronger magnets. Using a magnet strength of 50 Amp-m^2 reduces the expected nutation angles to between 5-10°. Source code from the modeling program has been included in Appendix 5-B.

Figure 5-14

Figure 5-15

5.2.4.2 Numerical Integration Simulation

A second simulation was created to numerically integrate the Equations of Motion (EOMs) describing SPARTNIK's attitude and also to fully visualize and understand the motion of SPARTNIK when in orbit. The goal of this model was threefold. The primary goal was to give some insight into whether the "spin" and "tumble" that SPARTNIK would experience in orbit would interact with each other, either by disrupting or canceling each other out. The fear being that, when spinning, SPARTNIK would act like a gyroscope and the induced tumble would interact with this spin and cause SPARTNIK to behave in an undesirable manner. The simulation would verify if this affect was indeed happening and if so what could be done to minimize it. The second goal was to resolve a problem with the moments of inertia of the satellite. It has been determined that extra mass is needed around the outside shell in order to make SPARTNIK spin about the Z-axis. The third and final goal of the simulation was to generate an attitude profile of SPARTNIK over the course of one orbit. Such profile could then be compared to the real attitude data once the satellite is in orbit.

With these objectives in mind it was determine to use MATLAB to numerically integrate the EOMs. Hereafter, the simulation mentioned above will be referred to as simply the simulation.

5.2.4.2.1 Definition of Frames/ Rotations

The first step to developing the simulation is to define a set of coordinates and coordinate frames in which the dynamic model will be developed. Three coordinate frames were chosen to model the dynamics of Spartnik: an inertial frame, a rotating frame, and a body fixed (also rotating) frame.

5.2.4.2.1.1 The Inertial (I) Frame X-Y-Z

The first frame defined is an inertial frame, labeled **X-Y-Z** and hereafter called simply the inertial frame. The origin is located at the center of the Earth with the **X** axis defined to point in the direction of the Vernal Equinox, **Z** pointing north and **Y** completing the right handed frame. This frame is used primarily to calculate the latitude and longitude of Spartnik's center of mass as it moves along its orbit. The process by which the spacecraft latitude and longitude are calculated is described later.

5.2.4.2.1.2 The Local Rotating (R) Frame x-y-z

Next a rotating frame, labeled **x-y-z** and hereafter referred to as simply the rotating frame**,** is defined with its origin centered on Spartnik's center of mass. The **x** axis points in the direction of motion in the plane of the orbit, **z** is nadir pointing (i.e. toward the center of the Earth), and **y** completes the right handed frame. Although this frame is defined with its origin at the center of mass and rotates around the orbital plane with Spartnik, it is *not* fixed in the body of the satellite. Therefore, the **z** axis will always be nadir pointing. The inertial and rotating frames are graphically depicted in Figure 5-16.

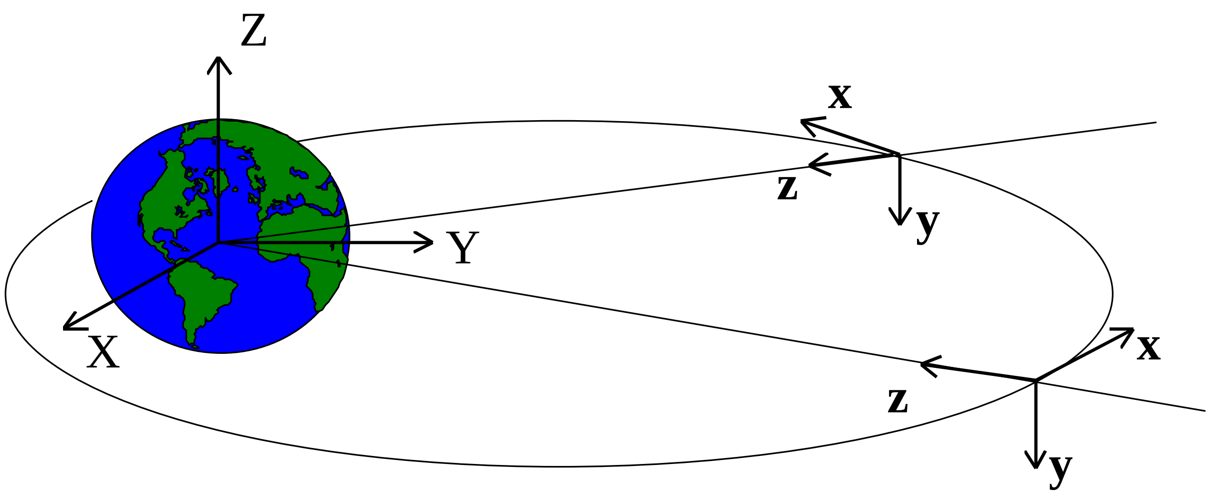

Figure 5-16: The Inertial and Rotating Frames

5.2.4.2.1.3 The Body (B) Frame b_1-b_2-b_3

A third frame, labeled $\mathbf{b_1}$-$\mathbf{b_2}$-$\mathbf{b_3}$ and hereafter called the body frame, is needed. The origin of this frame is centered on Spartnik's center of mass and is defined such that $\mathbf{b_1}$ points outward normal to Panel 3, $\mathbf{b_2}$ points outward normal to Panel 1 and $\mathbf{b_3}$ points outward normal to the top Panel. This frame is graphically represented below in Figure 5-17.

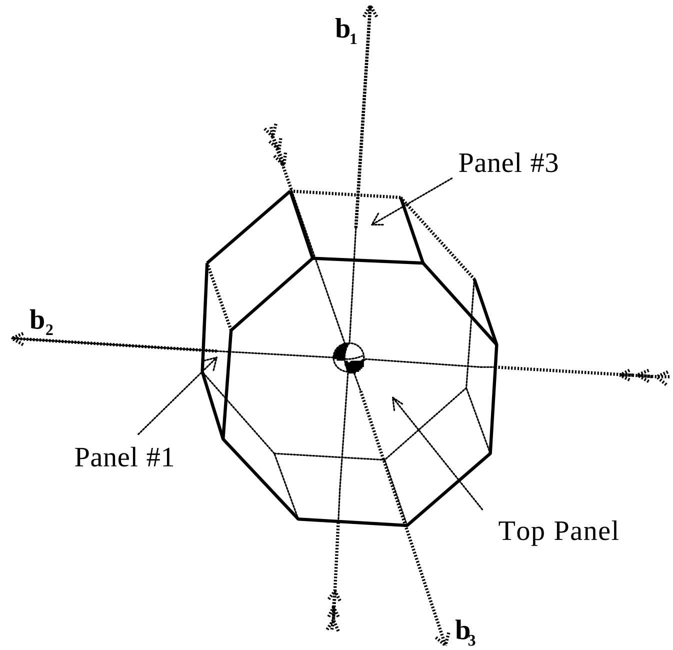

Figure 5-17: The Body Frame

The body frame is defined such that it is fixed in the body of Spartnik and thus will be used to determine the orientation of Spartnik with respect to the rotating frame. Since the **z** axis is always nadir pointing the offset of the $\mathbf{b_3}$ axis from nadir can easily be used to measure the performance of the attitude control system. If Spartnik's attitude control system is working as designed this offset angle will be small when over the northern hemisphere. Therefore, one of the primary goals of the simulation, namely whether the camera is pointed Earthward when over the northern hemisphere, can be determined quickly. The end goal of the simulation is to generate a time history of the orientation of the body frame with respect to the rotating frame.

In order to relate the rotating frame to the body frame a 1-2-3 body Euler rotation is performed. Initially, the body frame can be assumed to be aligned with the rotating frame, that is $\mathbf{b_1}$ aligned along the **x**-axis, $\mathbf{b_2}$ along the **y**-axis, and $\mathbf{b_3}$ along the **z**-axis. First, the body frame is pitched ϕ degrees about the **x** axis. Next, the resulting intermediate frame is pitched θ degrees about the **y'** axis and finally yawed ψ degrees about the **z"** axis. These three rotations, ϕ, θ and ψ, are shown in Figure 5-18.

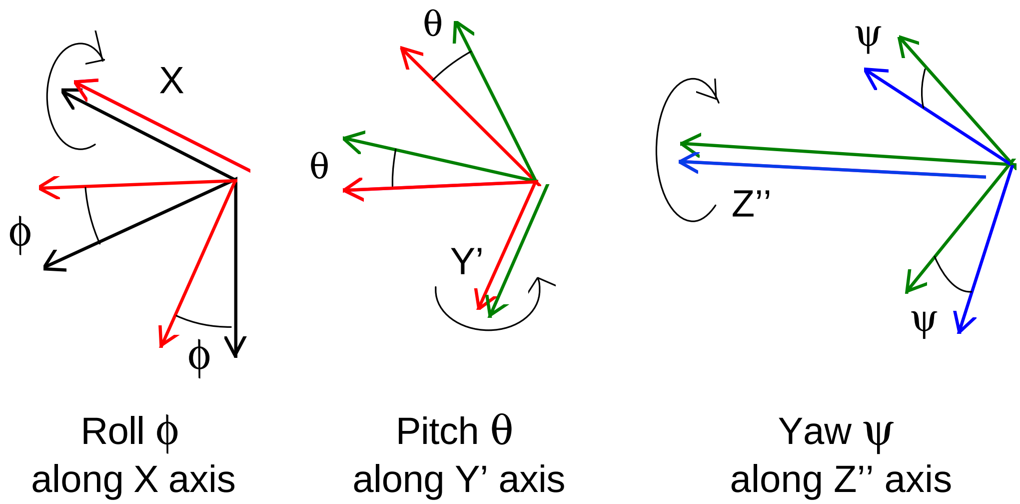

Figure 5-18: Body 1-2-3 Rotation

Combining the results of these three rotations leads to a direction cosine matrix allowing the transformation of any vector from the rotating frame to the body frame. The matrix becomes:

$$\begin{Bmatrix} \mathbf{b_1} \\ \mathbf{b_2} \\ \mathbf{b_3} \end{Bmatrix} = \begin{bmatrix} C_q C_y & S_f S_q C_y + C_f S_y & -C_f S_q C_y + S_f S_y \\ -C_q S_y & -S_f S_q S_f + C_f C_y & C_f S_q S_y + S_f C_y \\ S_q & -S_f C_q & C_f C_q \end{bmatrix} \begin{Bmatrix} \mathbf{x} \\ \mathbf{y} \\ \mathbf{z} \end{Bmatrix} \qquad \text{(Equation 5-14)}$$

5.2.4.2.2 Derivation of the Equations of Motion

With the frames defined, a means to rotate among them, and the objectives of the simulation in mind, the EOMs can now be derived. Numerical integration of these EOMs will give a time history of the orientation of Spartnik. A few assumptions are built into the simulation. First, an early estimate of the mass distribution of Spartnik generated the following moments of inertia:

Table 5-6: Estimated Moments of Inertia

$I_{xx} =$ 0.30393 kg·m^2	$I_{xy} =$ 0.00009 kg·m^2
$I_{yy} =$ 0.32415 kg·m^2	$I_{xz} =$ -0.00044 kg·m^2
$I_{zz} =$ 0.48614 kg·m^2	$I_{yz} =$ -0.00315 kg·m^2

Although these values are not finalized they show that the satellite's body axes, as defined previously, can be assumed to be along principle axes. This assumption allows the derivation of the EOMs to be simplified, using the fundamental equation from Newtonian mechanics

$$\mathbf{M} = \frac{{}^{I}d\mathbf{H}}{dt} = \frac{d}{dt}\left\{[I]^{\mathrm{I}}\mathrm{w}^{\mathrm{B}}\right\} \qquad \text{(Equation 5-15)}$$

where

$\mathbf{M}$	= sum of the external moments about the center of mass (N·m)
$^{I}d\mathbf{H}/dt$	= time derivative of the angular momentum about the center of mass relative to an inertial frame (kg·m^2/s)
[I]	= inertia matrix about the center of mass, assumed constant for Spartnik (kg·m^2)
$^{I}\mathrm{w}^{B}$	= angular velocity vector of the body frame relative to an inertial frame (radians/s)

Breaking down the overall equation into its different components using Euler's form of equation 5-15 gives

$$M_1 = I_{xx}\dot{w}_x + \left(I_{zz} - I_{yy}\right)w_y w_z \qquad \text{(Equation 5-16a)}$$

$$M_2 = I_{yy}\dot{w}_y + \left(I_{xx} - I_{zz}\right)w_x w_z \qquad \text{(Equation 5-16b)}$$

$$M_3 = I_{zz}\dot{w}_z + \left(I_{yy} - I_{zz}\right)w_x w_y \qquad \text{(Equation 5-16c)}$$

where

M_1 = sum of the externally applied moments about the **x**-axis (N·m)
M_2 = sum of the externally applied moments about the **y**-axis (N·m)
M_3 = sum of the externally applied moments about the **z**- axis (N·m)
I_{xx} = moment of inertia about the **x**-axis (kg·m^2)
I_{yy} = moment of inertia about the **y**-axis (kg·m^2)
I_{zz} = moment of inertia about the **z**-axis (kg·m^2)

Note I_{xy}, I_{xz}, and I_{yz} are approximated as zero.

Solving equations (5-16a), (5-16b), and (5-16c) for $\dot{w}_x$, $\dot{w}_y$, $\dot{w}_z$ leads to

$$\dot{w}_x = \left(\frac{1}{I_{xx}}\right)\left[M_x - \left(I_{zz} - I_{yy}\right)w_y w_z\right] \qquad \text{(Equation 5-17a)}$$

$$\dot{w}_y = \left(\frac{1}{I_{yy}}\right)\left[M_y - \left(I_{xx} - I_{zz}\right)w_x w_z\right] \qquad \text{(Equation 5-17b)}$$

$$\dot{w}_z = \left(\frac{1}{I_{zz}}\right)\left[M_z - \left(I_{yy} - I_{xx}\right)w_x w_y\right] \qquad \text{(Equation 5-17c)}$$

These equations are only valid if the angular velocity is described with respect to an inertial frame. The angular velocity of the body frame with respect to the inertial frame can be expressed as

$$ {}^{I}\mathrm{w}^{B} = {}^{I}\mathrm{w}^{R} + {}^{R}\mathrm{w}^{B} \qquad \text{(Equation 5-18)}$$

Expressed in body frame coordinates this becomes

$$ {}^{I}\mathrm{w}^{B} = w_x\mathbf{b_1} + w_y\mathbf{b_2} + w_z\mathbf{b_3} \qquad \text{(Equation 5-19)}$$

Assuming a circular polar orbit with constant orbital speed, the angular velocity of the rotating frame with respect to the inertial frame is simply

$$ {}^{I}\mathrm{w}^{R} = -n\mathbf{y} \qquad \text{(Equation 5-20)}$$

where "n" is the mean orbital motion equal to the angular rate of Spartnik moving on its orbit or

$$ n = \sqrt{\frac{m}{a^3}} \qquad \text{(Equation 5-21)}$$

where

μ = geocentric gravitational constant (3.986 x 10^5 km^3/sec^2)
a = semi-major axis of orbit (km)

Converting equation 5-20 into body frame coordinates using the direction cosine matrix from equation 5-14 leads to

$$ {}^{I}\mathrm{w}^{R} = \left(-nS_f S_q C_y - nC_f S_y\right)\mathbf{b_1} + \left(nS_f S_q S_y - nC_f C_y\right)\mathbf{b_2} + \left(nS_f C_y\right)\mathbf{b_3} \qquad \text{(Equation 5-22)}$$

The angular velocity of the body frame with respect to the rotating frame, ${}^{R}\mathrm{w}^{B}$, can be expressed as follows

$$ {}^{R}\mathrm{w}^{B} = \dot{f}\mathbf{x} + \dot{q}\mathbf{y''} + \dot{y}\mathbf{b_3} \qquad \text{(Equation 5-23)}$$

where $\dot{f}$, $\dot{q}$, and $\dot{y}$ are as described in Figure 5-18. This equation, expressed in the body frame, becomes

$$ {}^{R}\mathrm{w}^{B} = w_1\mathbf{b_1} + w_2\mathbf{b_2} + w_3\mathbf{b_3} \qquad \text{(Equation 5-24)}$$

where

$$ w_1 = \dot{q}\sin y + \dot{f}\cos q \cos y \qquad \text{(Equation 5-25a)}$$

$$ w_2 = \dot{q}\cos y - \dot{f}\cos q \sin y \qquad \text{(Equation 5-25b)}$$

$$w_3 = \dot{f}\sin q + \dot{y} \quad \text{(Equation 5-25c)}$$

Equation 5-23 gives an expression of the angular velocity of the body frame with respect to the rotating frame that can be (numerically) integrated with equation 5-17(a-c) once the external moment components M_x, M_y, M_z are specified. Substituting equations 5-19 and 5-22 into 5-18 and equating like-terms leads to the following three equations

$$w_1 = w_x + nS_f S_q C_y + nC_f S_y \quad \text{(Equation 5-26a)}$$

$$w_2 = w_y - nS_f S_q S_y + nC_f C_y \quad \text{(Equation 5-26b)}$$

$$w_3 = w_z - nS_f C_q \quad \text{(Equation 5-26c)}$$

Finally, solving equation 5-25(a-c) for $\dot{f}$, $\dot{q}$, and $\dot{y}$ leads to the following expressions for the angular velocities of Spartnik

$$\dot{f} = \left(\frac{C_y}{C_q}\right)w_1 - \left(\frac{S_y}{C_q}\right)w_2 \quad \text{(Equation 5-27a)}$$

$$\dot{q} = S_y w_1 + C_y w_2 \quad \text{(Equation 5-27b)}$$

$$\dot{y} = \left(\frac{-S_q C_y}{C_q}\right)w_1 + \left(\frac{S_q S_y}{C_q}\right)w_2 + w_3 \quad \text{(Equation 5-27c)}$$

Note that these expressions experience a singularity when θ equals 90 degrees. Additionally, θ is limited to a range of -90° to +90°. These final three equations, along with the three equations 5-17(a-c), can be numerically integrated to generate a time history of the orientation of Spartnik.

5.2.4.2.3 Modeling of External Moments

Once the equations of motion and coordinate frames are identified and defined the external moments that will be acting on Spartnik need to be identified and modeled. Spartnik will experience at least four different torques while in orbit. These torques result from aerodynamic drag, solar radiation pressure, gravity gradient, and magnetic field effects[5]. Calculations show that the magnetic field interaction is three orders of magnitude greater than the other three torques[6]. Therefore, it is the first external moment to be modeled.

5.2.4.2.3.1 Earth's Magnetic Field

In order to model the interaction of the permanent magnets with the Earth's magnetic field a reliable model for the Earth's magnetic field is needed. The field model used is the International Geomagnetic Reference Field (IGRF) model. This model includes the main or core field without external sources, such as the interaction of the field with the solar wind. The field model is valid for altitudes up to 30,000 kilometers and for the years 1945 to 2000[7]. Two sets of magnetic field data with different resolutions have been obtained. One is a 5° latitude by 5° longitude grid and the other is a 10° by 10° grid, both compiled for a 1000 km altitude. Simulations can be run using the 10° by 10° grid for the purpose of debugging the code. Once the bugs are fixed, and one obtains trustworthy results, the grid definition can be increased to 5° by 5° for more accurate results.

In order to obtain the field vector for longitude and latitude values that lie within the grid points bilinear interpolation is used. Reference 7 describes the interpolation method used in this simulation. A description of the core field and a single block of the downloaded grid are pictured in Figure 5-19.

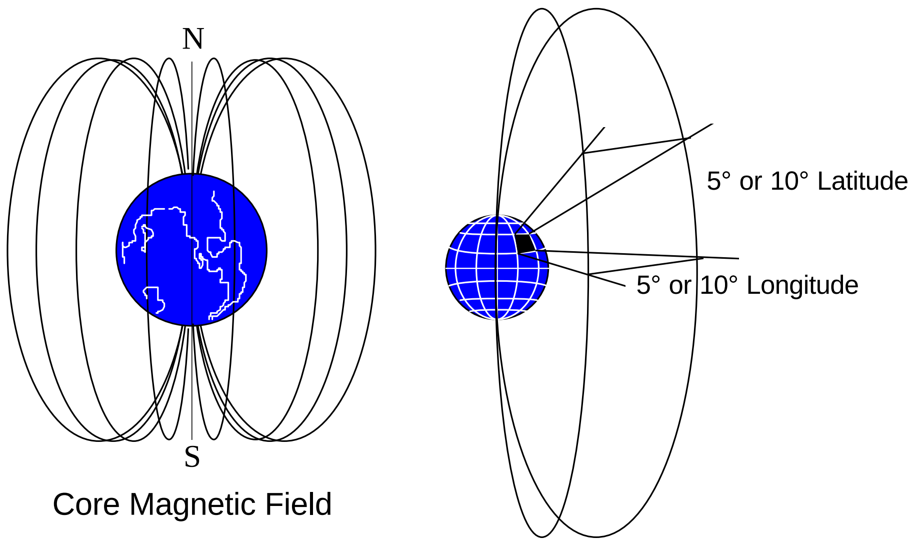

Figure 5-19: Core Magnetic Field and Sample of Data Grid

The moment due to the Earth's magnetic field can be modeled as

$$t = m \times \mathbf{B} \qquad \text{(Equation 5-28)}$$

where

t = resulting torque applied to Spartnik (dyne·cm)
m = magnetic dipole moment of Spartnik (EMU)
$\mathbf{B}$ = local magnetic field vector of Earth's magnetic field (Gauss)

The required magnetic dipole of the magnets on Spartnik have been preliminary estimated to be 5.2×10^3 EMU for two magnets, directed in the positive $\mathbf{b_3}$ direction. The strength of these magnets will not vary significantly within the life span of Spartnik due to their low demagnetization properties[8].

Now that both parameters for equation 5-28 are defined the torque that Spartnik will experience through its orbit due to the Earth's magnetic field and the permanent magnets can be computed by the process described below:

(1) Calculate the position of Spartnik on its orbit using Kepler's Equation.
(2) Compute the latitude and longitude of Spartnik's center of mass.
(3) Use the latitude, longitude, and bilinear interpolation to calculate the local magnetic field vector ($\mathbf{B}$).

(4) Calculate m. The direction of the vector, in the rotating frame, is determined by Spartnik's current orientation.

(5) Calculate t and integrate EOMs to get new orientation of Spartnik.

(Note $\mathbf{M} = t = M_1\mathbf{b_1} + M_2\mathbf{b_2} + M_3\mathbf{b_3}$)

5.2.4.2.4 Numerical Simulation Methodology

MATLAB was the chosen tool to numerically integrate the EOMs described above. The reason for this choice was ease of development and familiarity of the program by the authors. For the purpose of debugging the code the function "ode23" was used to numerically integrate the EOMs. Ode23 uses second and third order Runga-Kutta formulas to numerically integrate a system of ordinary differential equations. While debugging the code the tolerance of the integration was set at $1x10^{-6}$. When the simulation was fully debugged fourth and fifth order Runga-Kutta formulas were used with the "ode45" function call and the tolerance lowered to $1x10^{-12}$.

5.2.4.2.5 Results

One of the goals of the simulation is to determine if the passive control system, as initially designed, will perform as planned. If the passive control system does perform as planned then simulations can be performed to determine how well it works under a variety of conditions. If it does not perform as planned then simulations can be run under a variety of conditions with the goal of making recommendations on how to improve the passive control system design. If Spartnik performs as expected it should tumble about the **y** axis at a rate of 720 degrees per orbit or two complete tumbles per orbit. The rotating frame will complete one revolution per orbit. Therefore, Spartnik should complete one tumble per orbit *with respect to* the rotating frame. All simulations were run over a half of an orbit, beginning over the North Pole and ending near the South Pole. Thus, Spartnik should tumble (pitch) through 90 degrees in a quarter orbit. The spin rate (yaw) should be constant and reflected in the output as a line of constant, increasing slope equal to the spin rate. As described earlier the pitch offset (θ) of the body frame with respect to the rotating frame is limited to the range -90° to +90°. However, over a half orbit Spartnik should pitch through 180 degrees. Therefore, in order to describe orientations of the satellite when it has "tumbled" through more than 90 degrees a 180 degree change in roll (ϕ) is kinetically required. When this 180 degree change in ϕ occurs, at the equator, q will reach 90 degrees and then "rebound," rising back to zero.

With the equations of motion and the external moments defined, the MATLAB program was run through a series of verification checks to make sure the program was working correctly and free of bugs. As stated earlier, initially the simulation was run using ode23 with a tolerance of $1x10^{-6}$. After the bugs had been eliminated from the code the simulation was run using ode45 and the tolerance lowered in steps down to a final value of $1x10^{-12}$. Although it is possible to lower the tolerance even more, the authors felt that this might induce round-off errors that could significantly change the results due to the low step size. All results discussed below were computed using ode45 with a tolerance setting of $1x10^{-12}$.

5.2.4.2.5.1 Program Verification

Two simulations were run in order to verify the program was working correctly. The first involved setting the initial spin rate and magnet strengths to zero. This has the effect of simulating

Spartnik as inertially pointed in space. With no external torques Spartnik should remain inertially pointed. All initial conditions for this simulation were set to zero (i.e. $w_x = 0.0$, $w_y = 0.0$, $w_z = 0.0$, $\dot{f} = 0.0$, $\dot{q} = 0.0$, $\dot{y} = 0.0$). The results of this simulation are depicted in Figure 5-20a-d.

Error! Not a valid link.Error! Not a valid link. Error! Not a valid link.Error! Not a valid link.

Figure 5-20(a-d): First Program Verification Simulation

The results confirm that Spartnik remains inertially pointed throughout the simulation. The rotating frame, however, does not remain inertially pointed and rotates as Spartnik moves along its orbit with a speed equal to the mean motion along the negative y direction. Therefore, Spartnik will appear to rotate along the positive y direction with respect to the rotating frame. This can be seen in Figure 5-20b.

The second verification performed involved setting the magnet strength to its initial values as determined by the original control system design. This involved two magnets whose combined magnetic dipole is equal to 5.2×10^3 EMU. All other initial conditions, including spin rate, were set to zero (i.e. $w_x = 0.0$, $w_y = 0.0$, $w_z = 0.0$, $\dot{f} = 0.0$, $\dot{q} = 0.0$, $\dot{y} = 0.0$). The results of this simulation are depicted in Figure 5-21 (a-d).

The expected 90 degree tumble over a quarter orbit about the **y** axis can be seen in Figure 5-21b. The yaw, depicted in Figure 5-21c is nearly zero for most of the orbit, as expected and desired. Figure 5-21d, which records the offset from the local magnetic field vector, is a measure of how well Spartnik is "locked" onto the Earth's magnetic field. From this graph it can be seen that, although it wobbles a bit, the offset from the Earth's magnetic field remains small. The 180 degree change in roll, depicted in Figure 5-21a, can be seen when pitch reaches 90 degrees. This change occurs near the equator and after this point pitch (θ) begins to increase and roll (ϕ) remains constant at -180 degrees.

Error! Not a valid link.Error! Not a valid link.Error! Not a valid link.Error! Not a valid link.

Figure 5-21 (a-d): Second Program Verification Simulation

5.2.4.2.5.2 Gyroscopic Effect Simulations

With the simulation working as expected it was determined to investigate the gyroscopic effect and determine if the control system, as designed, would perform as desired. The next simulation performed involved setting the spin rate about the $\mathbf{b_3}$ axis to 0.5 revolutions per minute ($\dot{q}$ = 0.05236 radians/sec, all others zero) and magnet strength of 5.2×10^3 EMU. These conditions represent the steady state conditions that are desired in orbit with the current control system. The results of the simulation are summarized in Figure 5-22(a-d).

Error! Not a valid link.Error! Not a valid link.
Error! Not a valid link.Error! Not a valid link.

Figure 5-22 (a-d): Current Control System Simulation Results

As can be seen from Figure 5-22b Spartnik does *not* tumble the desired 90 degrees in a quarter orbit. The offset from the Earth's magnetic field, depicted in Figure 5-22d, grows unacceptably high. By the end of a quarter orbit the offset is over 25 degrees. This indicates that the gyroscopic effect is preventing Spartnik from locking onto the Earth's magnetic field and therefore not tumbling the desired amount.

The next series of simulations continued the investigation of the gyroscopic effect. The results depicted in Figure 5-22 (a-d) indicate that the magnets are either too weak to lock Spartnik onto the Earth's magnetic field, the satellite is spinning too fast, or, more probably, a combination of the two. Although simulations were run over a *half* orbit, the number of degrees tumbled in a *quarter* orbit will be used as the test for how well the system behaves. This is due to the complex motion in pitch and roll. Recall, the pitch should tumble through near 90 degrees over a quarter orbit and then "rebound". Over the next few simulations the spin rate was lowered incrementally until the magnets were able to tumble the satellite over 90 degrees in a quarter orbit. The results of these simulations are summarized below:

Table 5-7: Investigation of Spin Rate on Control System Performance

Error! Not a valid link.

For spin rates below 0.2 revolutions per minute the satellite tumbles the desired amount. Remember, because Spartnik may not be perfectly "locked" onto the Earth's magnetic field the satellite may not tumble through the complete 90 degrees in a quarter orbit. The total number of degrees may be less than 90 if the offset from the Earth's magnetic field is large. Nevertheless an offset from the Earth's magnetic field of under 10 degrees is acceptable for Spartnik. So, if the satellite tumbles through approximately 80 degrees in a quarter orbit it is assumed the passive control system is working correctly. At 0.2 revs/min the maximum offset from the Earth's magnetic field was 19 degrees.

5.2.4.2.5.3 Magnet Strength Simulations

The next series of simulations involved investigating the strength of the magnets and their effect on control system performance. Eight simulations were run each incrementing the number of magnets, and therefore, the total magnetic dipole magnitude. The spin rate for each of these simulations was set at 0.5 revolutions per minute. The results of these simulations are summarized below:

Table 5-8: Investigation of Magnet Dipole Strength on System Performance

Error! Not a valid link.

From Table 5-8 it can be seen that a total magnetic dipole of 1.04×10^4 EMU is required in order to overcome the gyroscopic effect induced by the 0.5 min/rev spin and cause Spartnik to tumble as desired. The maximum offset from the Earth's magnetic field vector was 12 degrees at this magnetic dipole strength. One interesting effect of increased magnetic dipole was an oscillation of the offset angle from the Earth's magnetic field. Because the magnetic dipole is so strong any offset from the Earth's magnetic field will cause a relatively large torque which, in turn, will quickly rotate the satellite in the direction of the field vector. The stronger the magnets the higher frequency this oscillation became.

5.2.4.2.5.4 Moments of Inertia Simulations

The final series of simulations run involved changing the moments of inertia in order to determine what effect this would have on the performance of the control system. The current design of Spartnik calls for ballast, in the form of metal plates, to be added to the outer shell of Spartnik in order to make I_{zz} the largest moment of inertia. However, the amount of ballast has yet to be determined. By varying the moments of inertia the simulation can provide some insight into the amount of ballast required for optimal performance of the control system under a variety of conditions. Moments of inertia are also difficult to determine precisely so information on how any possible errors in their calculation will affect the control system is also important.

During this series of simulations the spin rate was set at 0.5 revolutions per minute and the magnet dipole strength at 5.2×10^3 EMUs. The moment of inertia about the **z** axis (I_{zz}) was incrementally decreased from 0.331646 kg/m^4, corresponding to 1.4 times I_{yy}, to 0.23689 kg/m^4 corresponding to 1.1 times I_{yy}. I_{xx} and I_{yy} were held constant. The results of the simulation are summarized below:

Table 5-9: Investigation of Varying Moments of Inertia

Error! Not a valid link.

As I_{zz} decreases it is expected that the gyroscopic stiffness of the system should also decrease and the performance of the magnets and the system as a whole should increase. From the results of this simulation this appears to be happening. However, Spartnik never achieves the desired tumble of 90 degrees over a quarter orbit. Varying the moments of inertia does not have as strong an effect on the performance of the control system as does varying the magnet strength or the spin rate. However, these simulations provide useful information that will be needed when selecting the final design of the passive control system.

5.2.4.2.5.5 Modified Control System Design

The results of the simulations raise concerns about the current control system design for Spartnik. However, they also provide some insight into what changes are necessary to improve the control system and make it more robust. The three parameters, spin rate, moments of inertia, and magnet dipole strength, all interact and make finding a simple solution for the control system difficult. The most difficult of these parameters to control is the spin rate. The factors that determine spin rate, namely: area of solar pressure paddles, difference in reflectance of both sides, amount and size of hysteresis rods, are known. However, calculating an accurate and reliable spin rate is very difficult. Therefore, it seems reasonable to determine a control system by changing the magnet strength and moments of inertia to suit a wide range of possible spin rates. Any results gained by these simulations that would determine magnet strength and moments of inertia must be checked against other subsystems. If the magnets are made too strong they can interfere with computer memory and possibly communications. The addition of mass along the outer shell of Spartnik must be checked for size constraints.

Error! Not a valid link.Error! Not a valid link.
Error! Not a valid link.Error! Not a valid link.

Figure 5-23(a-d): Modified Control System Simulation Results

Taking the above factors into account a new control system was designed for Spartnik. The new design was driven by a need to overcome the gyroscopic effect while not knowing precisely what the final spin rate of Spartnik will be. Therefore, every effort was made to change the design to lower the gyroscopic stiffness. Specifically, the number of magnets was increased from 2 to 8 magnets, increasing the total magnetic dipole from $5.2\text{x}10^3$ EMU to $2.8\text{x}10^4$ EMU. The moment of inertia about the **z**-axis was lowered from an estimate of 1.5 times I_{yy} to 1.1 times I_{yy}. Finally, the difference between the reflective and absorptive sides of the solar pressure paddles will be changed in an attempt to lower the spin rate. A conservative estimate of the new spin rate is 0.4 rev/min, down from 0.5 rev/min. The results of this new control system design over a half orbit for a 1000 km altitude are depicted in Figure 5-23 (a-d). As can be seen from Figure 5-23b Spartnik tumbles through 90 degrees and then "rebounds" back towards zero. The offset from the Earth's magnetic field vector, depicted in Figure 5-23d, remains close to zero over the entire simulation indicating that Spartnik is "locked" onto the Earth's magnetic field. Finally, y remains close to zero when Spartnik is in the northern hemisphere. When q reaches 90°, y drops to -180° and remains there for the remainder of the simulation. Therefore, this control system design meets all the design requirements.

5.2.4.2.6 Conclusion

All the simulations described above were run at an altitude of 1000 km and in a polar orbit. Since the actual orbit of Spartnik may be lower than 1000 km the performance of the modified control system at lower altitudes is also needed. However, since the magnetic field drops off with altitude, one can assume that if the control system performs adequately at 1000 km, it will perform well at lower altitude. Additional investigations are needed for different inclinations.

Additionally, it must be remembered that any results gained by this simulation are just that, a simulation of reality. When Spartnik is in orbit there will be many more torques present, including solar pressure and gravity gradient torques. In addition, there will be dissipative forces that were not included in the simulation, including the hysteresis rods and the nutation damper; these will aid in the stabilization of Spartnik. These additional effects were unable to be included in this model due to time limitations. As mentioned earlier, the magnitudes of the torques described above will be orders of magnitude less than that of the magnets interaction with the Earth's magnetic field. However, their ultimate effect on the control system will be seen when Spartnik is launched into orbit.

5.3 Construction and Assembly

The following figure shows the corresponding placement for all of ADCS components. A construction procedure will follow explaining, at a high level, how to proceed in building the different components.

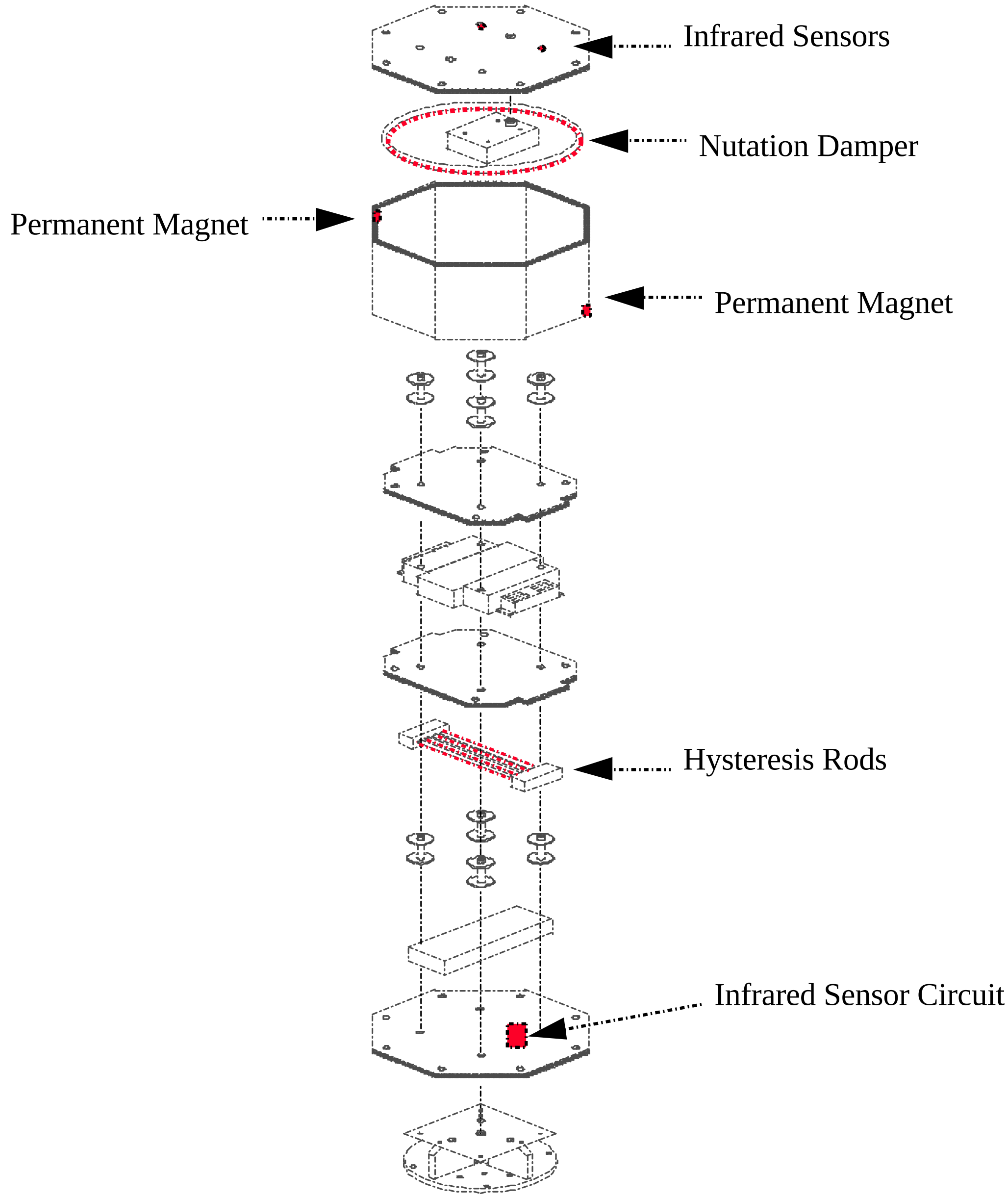

Figure 5-24 Placement of ADCS Hardware Components

5.3.1 Permanent Magnets

1. Construction does not apply for the permanent magnets but they must be integrated into SPARTNIK
2. The magnets will be placed into SPARTNIK's honeycomb side panels.
3. Panels must be opposite-facing
4. Magnets are pressed into triangular shaped section between honeycomb side panels, making sure that the poles are facing the correct direction.
5. Magnets' South poles face the +Z face, this is to insure the +Z face of spacecraft to be pointing towards the earth while orbiting on the northern hemisphere.
6. Once the magnets are inserted apply adhesive around magnet and let dry.

5.3.2 Solar Pressure Paddles

1. Obtain carpenter's measuring tape
2. Remove the unwanted painted surfaces
3. Cut tape to measure: short antenna, 17.5 cm and long antenna, 50.0 cm
4. Coat the concave side with aluminum coated tape with reflectance of q = 0.81
5. Anodized or paint, with a space-rated flat paint with reflectance of q = 0.03, the opposite side of the measuring tape.
6. Allow to dry and then proceed to mount the antennas in a stagger fashion; four on +Z face and four on the -Z face of the satellite.
7. Make sure that the alternating pattern of the antennas is followed across the +Z face and the -Z.

5.3.3 Hysteresis Rods

1. Obtain one 0.14125 inch steel rod of approximately 42 inches long. The rod must be made of 49% hyperm steel, and be hydrogen annealed.
2. The steel rod is then cut into 4 rods of 14 inches in length.
3. Insert each rod into the four holes on the side of the mounts, and apply adhesive to keep them from moving, yet giving them room to expand as needed.
4. Screw the rod-mounts along the bottom side of the power sub-system tray in the x-y plane, perpendicular to the spin axis.

5.3.4 Nutation Damper

1. Attach one side of the pressure seal as described below.
2. Place crimp bolt over one end of tubing. May have to work it down the tubing as it will be a tight fit.
3. Place washer over tubing.
4. Place fairing over tubing with narrow end in the direction of the cut end of the tubing. Make end of fairing flush with the end of tubing.
5. Attach connector to crimp bolt and finger tighten.
6. Bend tubing into circular shape, add oil, and repeat steps 2 through 5 for other crimp bolt.
7. After bolts are finger tightened, attempt to line up faces of connector and crimp bolts.
8. Turn both crimp bolts one additional face to tighten and crimp the fairing to the tubing.

5.3.5 Infrared Sensors

1. Construction of the infrared sensors does not apply here.
2. Obtain two infrared sensors from Radio Shack (part # 276-145).
3. Insert sensors into the provided holes in the +Z face of the satellite. Make sure to insert them from the inside of the satellite.
4. Add adhesive and let dry.
5. Connect their leads to the respective wires provided by the power subsystem.

5.4 Testing

5.4.1 Infrared Sensors

As mentioned earlier the primary function of the infrared sensors is to detect when the top (+Z) face of SPARTNIK is pointed towards the Earth. A preliminary test was conducted to determine the aperture of the sensors. The results of this test indicated that the sensor's field of view was so broad that the sensors will register an “on” reading possibly while detecting more than just the Earth. The results of this test are shown in Figure 5-25.

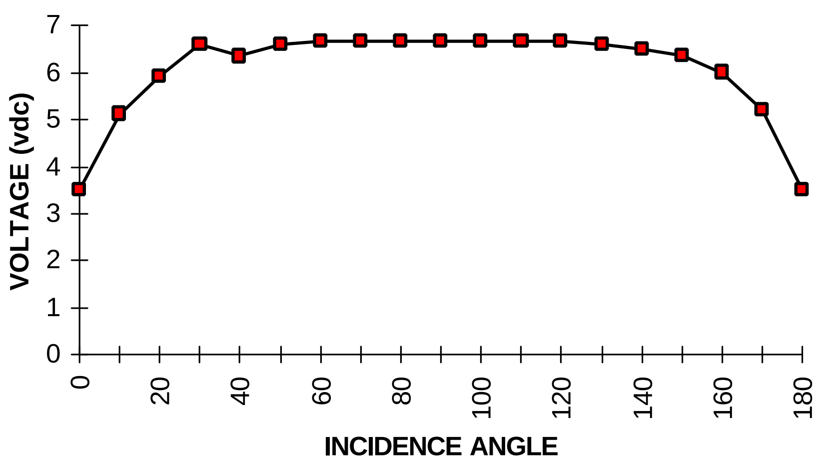

Figure 5-25 Infrared Detector Field of View

From this graph it is evident that mounting considerations had to be looked at carefully to limit the field of view of the detectors and additional testing was needed. To obtain better results, the sensors were tested in a "mock-up" model of SPARTNIK where the detectors were placed into the structure with an aperture of 5.5 mm in diameter. Figure 5-26 shows that the sensors output will allow for binary on and off readings but the field of view is still too large and may give erroneous readings which may indicate Earth pointing. Alternate positioning of the sensor such as recessing the detector further back into the aperture gave similar results and did not narrow the detector's field of view.

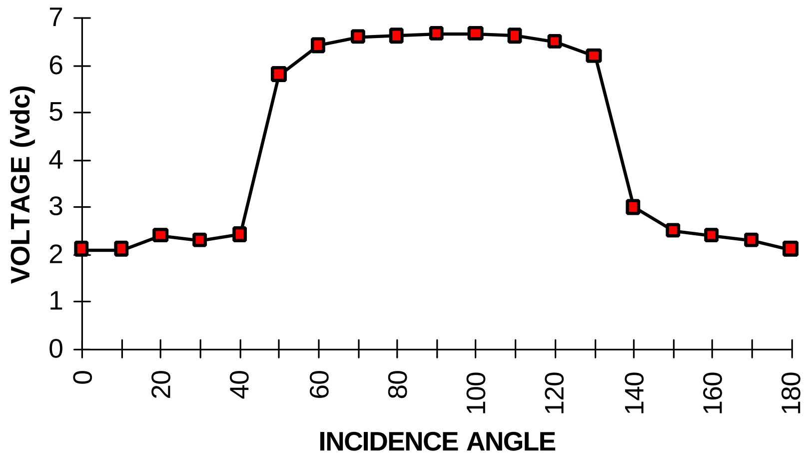

Figure 5-26 Infrared Detector Field of View (5.5 mm aperture)

The next set of tests included limiting the field of view the sensor samples through the top face of the spacecraft. This was done by decreasing the diameter of the aperture to 2 mm and 1.6 mm. The results from both test cases allowed the sensor the ability to take on and off readings while narrowing the field of view of each detector. Figure 5-27 and Figure 5-28 show the sensors field of view totaling approximately 40 degrees. It is reasonable to assume that with the sensors mounted in this way, the Earth will be the only body able to cause a maximum output from both detectors simultaneously. Additional results of testing are located in Appendix 5-E.

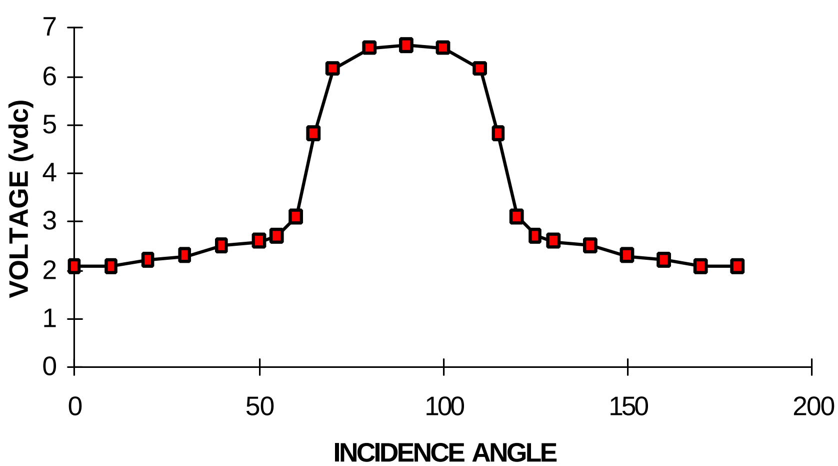

Figure 5-27 Infrared Detector Field of View (2 mm aperture)

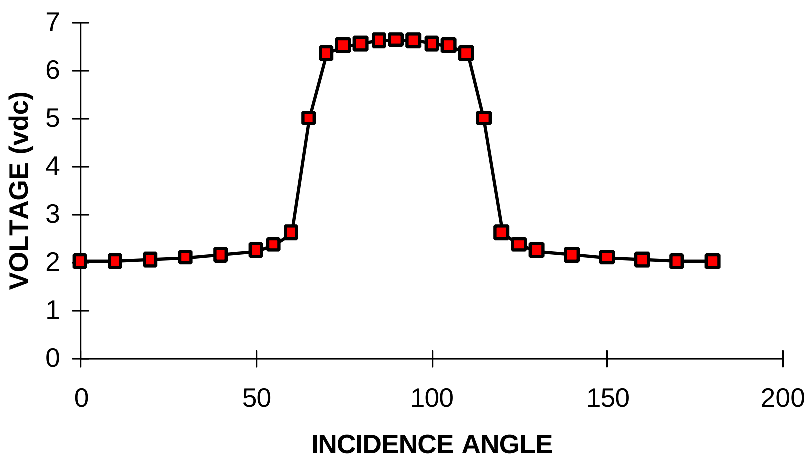

Figure 5-28 Infrared Detector Field of View (1.6 mm aperture)

5.4.2 Attitude Determination Algorithm Status

The attitude determination algorithm has been coded in C language for use at the ground station. A listing of the source code is in the appendix. The program currently obtains a vector from the satellite body fixed frame to the sun by using statistical analysis of current readings obtained from the solar arrays. It also calculates the Earth's position with respect to the Sun given date and time information. The algorithm calculates the Earth's current orbital elements. These elements are used to calculate a vector from the Earth to the sun. The algorithm also transforms this vector into the local vertical frame of the satellite given current position information. This gives us two sun vectors in different frames, which can be compared to obtain Euler angles.

We will need to calculate the satellite's orbital elements from information provided by NORAD. The algorithm is capable of autonomously calibrating itself daily. This is accomplished by taking a time history of daily maximum current outputs from the solar arrays. These values are reset daily using a one day service routine. Values from the previous day will be used as the present calibration factor. This autonomous calibration will cancel adverse effects such as cell degradation.

The attitude determination algorithm has been tested to show that sample current readings match well with expected sun vector orientation. Also for a given date and time the algorithm calculates orbital elements of the Earth as well as the Earth-Sun vector that compare nicely with values given in the current Astronomical Almanac[9]. The algorithm also calculates Julian date from standard date and time, this also has been shown to be very accurate. Some examples of the attitude determination program test cases are shown in Table 5-10. Additional test cases are given in Appendix 5-F. The first and second columns show the calendar and Julian dates used in the calculation. The third and fourth columns list the Mean Longitude and Mean Anomaly of the Earth with respect to the Sun in the inertial frame. The last three columns show the X, Y, and Z components of the vector from the Earth center to the Sun center in the Earth fixed reference frame.

Sample current sensor data used to test output of the algorithm is developed by a cosine relationship of the variation of output with respect to incidence angle. The current readings will be calibrated on board the spacecraft thus giving normalized values between one and zero for output magnitude. Readings of 1.0 will correspond to the maximum current output generated during the previous day for that particular solar panel and thus an incidence perpendicular to the solar array. Sensors that are shadowed from the sun are given a zero value.

By editing the header file that contains the solar panel current data (sendat.h), the current values for each solar panel was entered for a corresponding expected value of Theta. With the value of Phi being held constant at 90°, the expected values were compared with the actual output of the algorithm. For the expected values contained in the spreadsheet found in Appendix 5-F, Theta was calculated to within 5 percent of the actual values.

Once the expected values of Theta were verified, the values for Phi were varied to determine the correlation between the combined values for Theta and Phi, and the resulting current values for the sensors. It was found that the test values used were accurate to within 5 percent as well. The only instances in which the algorithm will not compute Theta and Phi was determined to be when the sun vector is normal to one of the faces of the spacecraft. This situation causes the current values for calculating Theta to be present in only three panels.(ie. Theta = 0°, 45°, 90°, ...) In this situation, the algorithm displays an error in using the arcsin function. The algorithm does compile for those certain values of Theta when Phi is set to the following values: 0°, 30°, 45°, 60°, and 90°. The algorithm is now being looked at by the software sub-system in order to determine the cause of this error.

Sample Current Sensor Data (Normalized)
AMPS11 = .7128, AMPS12 = .3528, AMPS21 = .504, AMPS22 = .252, AMPS31 = 0.0, AMPS32 = 0.0, AMPS41 = 0.0, AMPS42 = 0.0, AMPS51 = 0.0, AMPS52 = 0.0, AMPS61 = 0.0, AMPS62 = 0.0, AMPS 71 = 0.0, AMPS72 = 0.0, AMPS81 = 0.504, AMPS82 = 0.252, AMPS91 = .70, AMPS95 = .35, AMPS103 = 0.0, AMPS107 = 0.0 };
ALGORITHM OUTPUT:
PANEL#1: angle1: 86.49 angle2: 93.51
PANEL#2: angle1: 359.89 angle2: 90.11
PANEL#8: angle1: 89.89 angle2: 180.11
ALGORITHM OUTPUT:
theta = 90.00 phi = 45.57 x = 0.00000 y = 0.714143 z = 0.700000

Table 5-10 Comparison Data for ADCS Algorithm

	DATE	**Julian Date**	**Mean Longitude**	**Mean Anomaly**	**X**	**Y**	**Z**
Almanac	Jan 03, 1995	2449720.5	102.223	359.331	-0.2078	0.8818	0.3823
Algorithm	Jan 03, 1995	2449720.5	102.152	359.300	-0.2066	0.8820	0.3824
Almanac	July 22, 1995	2449920.5	299.342	196.350	0.4897	-0.8168	-0.3541
Algorithm	July 22, 1995	2449920.5	299.281	196.420	0.4887	-0.8172	-0.3543

The attitude determination program can be expanded upon to include the prediction of orbital elements of the satellite. It could also include information about the Earth's magnetic field for prediction of the orientation of the spacecraft's magnetic dipole.

5.5 Operations

5.5.1 Definition Of ADCS Control Modes

SPARTNIK's ADCS subsystem is designed to operate under different control modes. For SPARTNIK, these are divided into the following categories; orbit insertion, acquisition, normal/on-station, slew, and contingency or safe.

5.5.1.1 Orbit Insertion

This is the period during which the spacecraft has left the launch vehicle and is brought into its final orbit. On more traditional missions, this mode has actuation options which include no control, spin stabilization, and full 3-axis control. Since the SPARTNIK project involves launching as a secondary payload on any number of launch vehicles, the final orbit is not yet determined.

At this time, being unsure of the final orbit into which we will be launched has placed an extensive requirement on the ADCS sub-system. Uncertainty in the final orbit requires the design of a system that can be used in a range of orbits, or can be tailored, with minor changes, to fit the final orbit. SPARTNIK's final orbit will be totally launch vehicle dependent.

5.5.1.2 Initial Acquisition

This mode involves the initial stabilization and attitude determination of the spacecraft. The worst possible case of initial tip-off rates for SPARTNIK, after separation based on information from industry mentors, is assumed to be as high as 5 °/sec. Initial stabilization will be of primary importance to the success of this project. Requirements include: arresting of tip-off rates induced from the launch vehicle release mechanism, and obtaining the initial spacecraft attitude determination.

5.5.1.3 Normal/On-Station

On-station will be the mode in which the spacecraft will operate throughout most of its lifetime. SPARTNIK will operate in the on-station mode for the majority of its two year predicted lifetime. The following requirements have been the driving force in this design: knowledge of the CCD orientation with a 5-10º accuracy including determination and errors, knowledge of the orientation of the Micro-Meteorite Impact Detector (MMI) within 5-10º, and the use of Earth horizon sensors to allow for the CCD to take photographs of Earth.

5.5.1.4 Slew

This mode requires that the spacecraft be reoriented as needed. It has been determined that the ability to change the spacecraft orientation manually would be of interest to our payload sub-system for obtaining a wider variety of CCD images. SPARTNIK's passive control system is unable to incorporate this ability, but preliminary research into an active control system has been done to show that this capability can be integrated into future projects.

5.5.1.5 Contingency Or Safe

This mode is used in case of emergency or primary control system failure. This mode could potentially consist of a system that requires less power than the primary control system or be completely separate from the main system. SPARTNIK has no alternate control system for stabilizing the spacecraft. The attitude determination portion of this sub-system, on the other hand, does utilize redundant systems.

5.5.2 ADCS Mission Procedures

The ADCS mission objective for SPARTNIK will be to measure and calculate any attitude or body axis rates of the satellite at different stages in its mission life and to predict, using data and computer simulation, future attitude and body axis rates. By enabling the ground station to calculate these occurrences we can determine attitude and predict when to take pictures for best results. Once the spacecraft is placed into its orbit, it will be necessary for the spacecraft to reach its prescribed two tumbles per orbit rate and its estimated two minutes per revolution spin rate. To understand how the spacecraft will function while in orbit, several factors must be considered. These factors include Initial Attitude Acquisition, an on orbit duty cycle, and contingency operation.

5.5.2.1 Initial Attitude Acquisition

The Initial Attitude Acquisition requires a majority of the ADCS subsystem focus since it is the first and most important stage to be experienced by SPARTNIK. This acquisition refers to procedures that will be followed once the satellite is placed into orbit. Since the satellite will have an undetermined attitude and unknown body axis rates once ejected from the launch vehicle, it is necessary to provide accurate measurements of these values in order to determine if SPARTNIK's passive control system is functioning as desired.

The first procedure to be performed is determining the ADCS sub-system status. This procedure will basically obtain a health status from all ADCS components and related sensors. It is important to determine whether we are receiving any information recorded by our sensors. Sensor readings from the solar panels and Earth horizon sensors will assist ADCS in determining SPARTNIK's attitude and tip-off rates from the launch vehicle. The conversion of ADCS sensor readings into attitude readings will be covered by the attitude determination algorithm discussed in the following section. Tip-off rates from launch vehicle can be as high as five degrees per second[1]; therefore, it is imperative that we stabilize the body axis rates of SPARTNIK to an acceptable rate.

5.5.2.2 Attitude Determination Algorithm

The attitude determination algorithm is important for gathering data on actual spin and tumble rates as well as indicating when the spacecraft will be in favorable orientations for picture taking. Portions of the attitude determination algorithm will be split between the ground station and the onboard SPARTNIK computers. The infrared sensors will allow the on-board computer to make autonomous decisions about when it is possible to take useful pictures. Determining the attitude of the spacecraft will be done by combining readings from the solar panel current readings, and infrared radiation sensors.

Readings from the solar panel current sensors will be used to determine the direction of the sun vector to a reference frame fixed in the spacecraft. The sun vector will determine two degrees of orientation with respect to the sun, leaving one degree of uncertainty about the sun vector. This means that the satellite could be rotated to any orientation about its sun vector and still read out the same spacecraft-sun orientation. This third degree of freedom will need to be resolved using another means of attitude determination.

The third degree of orientation can be determined in either of two ways: by predicting the position of the spacecraft in orbit, or with readings from the IR sensors. With knowledge of the spacecraft's position in orbit using orbital equations, the instantaneous magnetic field vector can be predicted. The SPARTNIK orbital position will be uplinked to the ground station computer from Keplerian data, which is either calculated or obtained from NORAD. Since one axis of the spacecraft will be held near this direction by the permanent bar magnets, the one degree of uncertainty will be resolved. In addition, the IR sensor readings will indicate when the spacecraft is oriented towards the Earth. This data will also be used to resolve the third degree of freedom when a redundant attitude determination is requested.

The solar panel current data will be the primary source of spin and tumble rates. This information will be used to determine effectiveness of thermal energy dissipation as well as predicting Earth pointing duration and actual magnetic field interaction. Considering a target spin rate of two minutes per revolution, solar panel current data will be taken every thirty seconds. This sample rate will be variable up to one reading every five seconds for use during initial attitude acquisition determination and also to check for false rate information caused by aliasing. Each of the spacecraft's solar arrays is composed of four strings of GaAs solar cells. Two of these strings on each solar array will have the current monitored by the on-board computer. This current data will be used by the ADCS algorithm.

The infrared sensor readings will be the primary source of Earth pointing determination. The readings from the infrared sensors will only be used with the attitude determination algorithm for redundancy because the Earth's wide field of view introduces less accuracy in resolving the third degree of freedom. The infrared sensor readings will be more useful for simply verifying Earth pointing for picture taking. These sensors register an "on" reading when pointed to the Sun, Moon, or Earth and an "off" reading when pointed into space. Earth is the only body with a wide enough field of view to activate more than one sensor at a time, therefore indicating Earth pointing. Due to the binary operation of the Earth Horizon Sensor, it will only indicate Earth pointing within 40° which is the sensors combined field of view. This uncertainty will be reduced by the knowledge of the spacecraft orbital position and the magnetic interaction between SPARTNIK and the Earth.

The sun vector will be determined using solar panel current readings with respect to readings from other solar panels. Current sensors were chosen over voltage sensors because variations in current output of the solar panels are more responsive to the incidence angle of a light source. The solar panel current readings follow a simple cosine law of current output magnitude with respect to incidence angle.

Figure 5-29 shows the method in which the sun angles will be related to a reference frame fixed in the spacecraft. The attitude determination algorithm will call for current readings from all panels, which will translate to angles from the calibrated curve fit equation. Each panel will be associated with a range of angles, which are measured with respect to the spacecraft fixed frame. The side panel ranges are as follows:

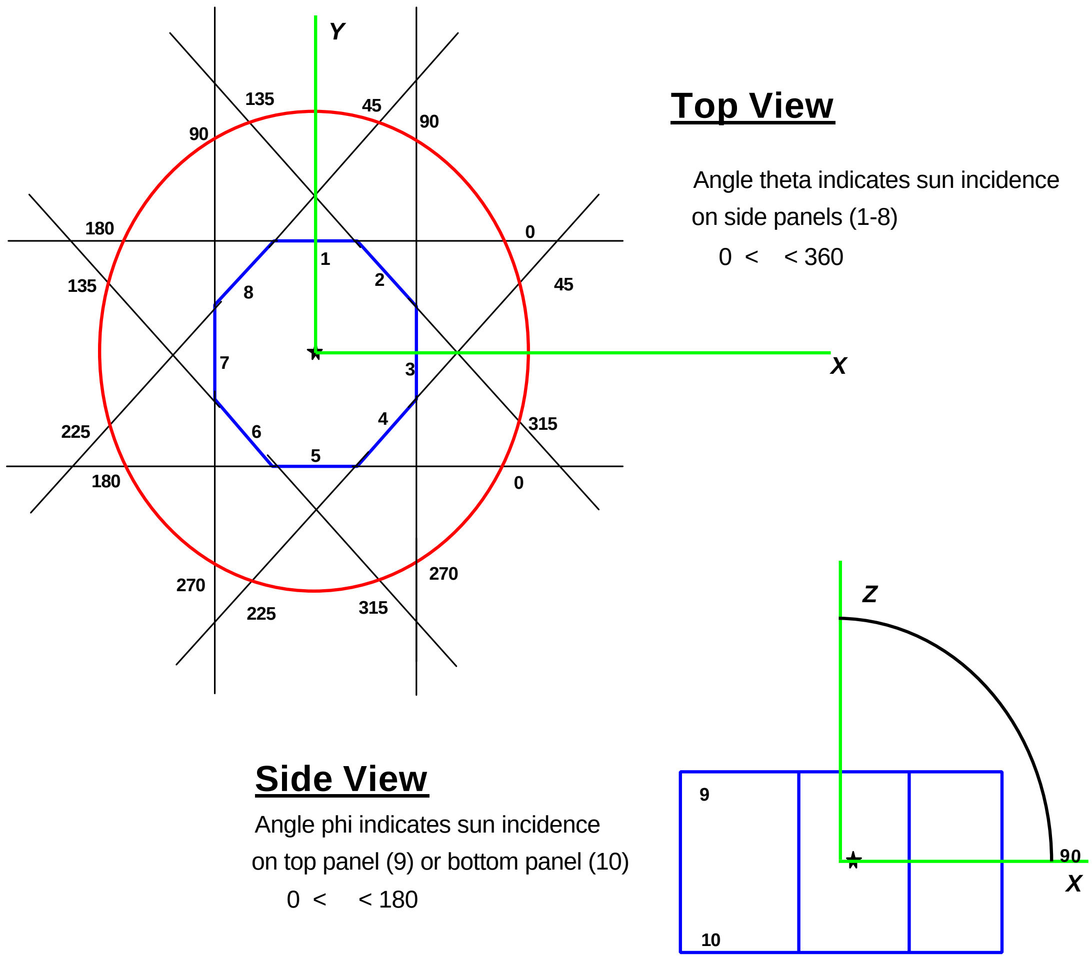

Figure 5-29 Sun Vector Determination

Table 5-11 Angle Range Designations by Panel

	Angle Range
Panel 1:	0° - 180°
Panel 2:	315° - 135°
Panel 3:	270° - 90°
Panel 4:	225° - 45°
Panel 5:	180° - 0°
Panel 6:	135° - 315°
Panel 7:	90° - 270°
Panel 8:	45° - 225°

When the sun is incident on the side panels, the sides with the top three current readings can be compared. Each side panel will have two possible angles that would give the same current reading. This uncertainty can be resolved by comparing readings from adjacent panels. Since the sides are set with appropriate ranges, the two angles that match from adjacent sides will determine the true angle. The angle between the incident sun vector on the side panels and the x-axis will be theta (Θ).

Phi (Φ), the angle measured from the positive z-axis to the negative z-axis will be easier to determine because it only ranges from 0° to 180°. This means that for a given current reading there can be only one angle. Phi will be calculated entirely from the current readings of either the top or bottom panels.

Using theta and phi, a unit sun vector with respect to the spacecraft fixed frame can be calculated. This is done simply by the following equations:

$$\hat{\boldsymbol{x}} = \sin(f)\cos(q) \qquad \text{(Equation 5-29)}$$

$$\hat{\boldsymbol{y}} = \sin(f)\sin(q) \qquad \text{(Equation 5-30)}$$

$$\hat{\boldsymbol{z}} = \cos(f) \qquad \text{(Equation 5-31)}$$

This sun vector gives the spacecraft orientation with respect to the sun, with only one degree on uncertainty.

In order to know the spacecraft orientation with respect to the Earth, one axis of the spacecraft must be determined in an Earth fixed reference frame. This is done by aligning the permanent bar magnet dipoles with the spacecraft's positive z-axis. These bar magnets will keep the spacecraft spin axis close to the orientation of the Earth's magnetic field vector. Because prediction of the Earth's magnetic field vector orientation is possible, the spacecraft orientation with respect to the Earth will be determined about all three axes.

Prediction of the Earth's magnetic field vector orientation, will require knowledge of the spacecraft's position in orbit. The only position information that will be required is latitude, longitude, and altitude. Orbital equations can be used to predict these values over several orbits before updated elements can be acquired from NORAD.

The attitude determination algorithm will need to be able to send and receive signals from the camera as well as the ground station. All raw data read from the sensors will be sent to the ground station upon request for telemetry analysis. IR sensors must be coordinated with the camera to ensure Earth pointing information is provided upon request by the camera or the ground station.

A high level outline of the algorithm is as follows:

1) Take readings from all 20 solar panel current sensors.
2) Execute panel health status report, flag erroneous readings to be ignored.
    i) Compare current readings of sensors on same panel
    ii) If %error between readings is greater than %10, flag error.
    iii) Use readings from sensors with highest current magnitudes.
3) Average sensor readings from each of ten panels to obtain panel current readings.
4) Rank panels #1 - #8 (Side panels) from highest current magnitude to lowest.
5) Verify that top three readings are from adjacent panels, if not flag error.
    i) Assign side with highest panel reading as the primary panel.
    ii) If second highest panel reading is adjacent to the primary panel assign it as the secondary panel.
    iii) If it is not adjacent, flag error and disregard panel.
    iv) Continue until three representative panels are chosen.
6) Calculate theta (Θ) from top three panels and compare values.
    i) Calculate difference between top three panel readings and their corresponding opposite side panel readings. (i.e. Panel #1 - Panel #5).
    ii) Use normalized current value with curve-fit equation developed during calibration to calculate two corresponding incidence angles.
    iii) Add appropriate angle to place particular panel angles within their defined output range. (i.e. panel #7 + 90^{o}).
    iv) Compare six angle values to determine true theta.
        a) Find the three panel angles with closest correlation.
        b) Calculate % error between three panel angles.
        c) If % error is large disregard angle, flag error.
        d) Set theta to average of remaining panel angles.
7) Rank panels #9 & #10 (top & bottom panels), set largest reading as primary panel.
8) Calculate phi (Φ) from primary panel, using curve-fit equation.

9) Calculate sun unit vector in spacecraft frame using equations 5-26, 5-27, and 5-28 which are repeated here:

$$\hat{\boldsymbol{x}} = \sin(f)\cos(q)$$

$$\hat{\boldsymbol{y}} = \sin(f)\sin(q)$$

$$\hat{\boldsymbol{z}} = \cos(f)$$

10) Access orbital equation function to obtain current Earth with respect to the Sun vector. (i.e. Earth_Sun(DATE, TIME) --> returns current vector).
11) Set sun unit vector in spacecraft frame equal to Earth_Sun vector, solve for transformation angles η, λ, and β.
12) Express satellite orientation in Earth inertial coordinates using transformation angles.
13) Access orbital prediction function to find current latitude, longitude, and altitude. (i.e. Sat_Pos(DATE, TIME) --> returns position information which is periodically updated by NORAD).
14) Access magnetic field vector function to obtain local vector orientation. (i.e. Earth_Mag(LATITUDE) --> returns local vector).
15) Compare magnetic field vector to the satellite spin axis (z) vector.
    i) Compare vectors to resolve quadrant uncertainty.
    ii) Take dot product of vectors to calculate nutation angle.
16) Take readings from 2 infrared radiation sensors.
    i) If both sensors register "on", set Earth Pointing == 1.
    ii) If not, set Earth Pointing == 0.
    iii) Earth Pointing must be accessible by camera and ground station.
17) Record and time stamp data collected for current program cycle.
18) Down-link attitude data once per orbit or upon request.

The algorithm described above will be contained at the ground station. Processing of the infrared sensors on-board is necessary, in order to communicate directly with the camera. Spin and tumble rates will be processed on the ground.

5.5.2.2.1 Current Sensors

The SPARTNIK micro-satellite will utilize the current readings from the solar arrays on the spacecraft sides panels #1 - #8 and on the top panel #9 and bottom #10. These readings will be used for determining spacecraft's attitude with respect to the Earth. These current readings, coupled with the time-of-illumination (TI) for each panel, will also be used for determining spacecraft pitch, roll, and yaw rates. It is necessary for each individual solar array to be calibrated before launch to determine the output as a function of solar ray incidence, I=I(a). Unfortunately, due to the delicate nature of the solar arrays, we must rely on calibration data performed on Silicon test cells rather than the Gallium Arsenide flight cells. The Gallium

Arsenide cells will be calibrated at a later date, when the actual flight model of the spacecraft is ready for construction. The spacecraft attitude will be resolved as follows:

1) The CPU will monitor solar array output and store data for future processing or forward the data for download to the ground station.

2) From the solar array current data, all sides having a zero reading will be discarded since this requires that there is little or no illumination of that panel. Therefore, it is known that the particular panel is facing away from the sun, relatively speaking.

3) Based on the remaining data and the original solar array calibration data, the beta angle, or angle the solar ray makes with the panel, can be determined. Given that we determine the beta angle with respect to three of the eight sides panels of the spacecraft, the attitude of the spacecraft with respect to the Earth-Sun vector can be resolved.

With additional information, the spacecraft pitch, roll, and yaw rates may also be determined as follows:

1) The CPU will monitor the solar array current and the time of illumination for each panel.

2) Based on this data, we will be able to identify any panel(s) that have constant or relatively constant output over time. We then can get a good idea of whether the spacecraft is rotating about the axis perpendicular to these constant current panels.

3) Remaining data will allow us to resolve the illumination periods into rotational rates. Additionally, flying permanent magnets as part of the attitude control system will cause the spacecraft to align with the dipole of the Earth's magnetic field. This alignment will assist with reducing the pitch rate to 2 revolutions per orbit, and will reduce the yaw rate as well.

5.6 Conclusion

The vast majority of the design, analysis and construction of the ADCS subsystem is complete. There are, however, two major areas that still need further work. First, the ADCS components need to be integrated into the flight vehicle. The method to install most of the components has been completed by previous classes. However, a method of attaching the hysterisis rods still needs to be developed.

Finally, the attitude determination code needs to be calibrated with the solar arrays when the final flight model is fully assembled. The attitude determination algorithm requires current readings from SPARTNIK's solar arrays. Therefore, the peak current generation for each solar array needs to be determined.

5.7 References

[1] Larson, W.J. and Wertz, J.R., (editors) *Space Mission Analysis and Design*, Microcosm, Inc., Torrance, CA and Kluwer Academic Publishers, The Netherlands, 1992

[2] Bonsall, Charles A., (editor) *Webersat Users Handbook*, Weber State University, 1991

[3] Wertz, J.R. (editor) *Spacecraft Attitude Determination and Control*, D. Reidel Publishing Co, 1978.

[4] Swartwout, M. *SAPPHIRE Preliminary Design Report*, Stanford Aero/Astro Department, Stanford, 1994

[5] Wertz

[6] SJSU FDR

[7] Web Site

[8] Dexter Catalog

[9] Nautical Almanac Office, United States Naval Observatory, *The Astronomical Alamanc for the year 1995*, United States Printing Office, 1994.